Conversion of *Helicobacter pylori* CagA from senescence inducer to oncogenic driver through polarity-dependent regulation of p21

Yasuhiro Saito,[1,2] Naoko Murata-Kamiya,[1] Toshiya Hirayama,[4] Yusuke Ohba,[3] and Masanori Hatakeyama[1]

[1]Division of Microbiology, Graduate School of Medicine, University of Tokyo, Tokyo 113-0033, Japan
[2]Division of Chemistry, Graduate School of Science, and [3]Laboratory of Pathophysiology and Signal Transduction, Graduate School of Medicine, Hokkaido University, Sapporo 060-0815, Japan
[4]Department of Bacteriology, Institute of Tropical Medicine, Nagasaki University, Nagasaki 852-8523, Japan

The *Helicobacter pylori* CagA bacterial oncoprotein plays a critical role in gastric carcinogenesis. Upon delivery into epithelial cells, CagA causes loss of polarity and activates aberrant Erk signaling. We show that CagA-induced Erk activation results in senescence and mitogenesis in nonpolarized and polarized epithelial cells, respectively. In nonpolarized epithelial cells, Erk activation results in oncogenic stress, up-regulation of the $p21^{Waf1/Cip1}$ cyclin-dependent kinase inhibitor, and induction of senescence. In polarized epithelial cells, CagA-driven Erk signals prevent $p21^{Waf1/Cip1}$ expression by activating a guanine nucleotide exchange factor–H1–RhoA–RhoA-associated kinase–c-Myc pathway. The microRNAs miR-17 and miR-20a, induced by c-Myc, are needed to suppress $p21^{Waf1/Cip1}$ expression. CagA also drives an epithelial–mesenchymal transition in polarized epithelial cells. These findings suggest that CagA exploits a polarity-signaling pathway to induce oncogenesis.

CORRESPONDENCE
Masanori Hatakeyama:
mhata@m.u-tokyo.ac.jp

Abbreviations used: CDK, cyclin-dependent kinase; CM, CagA-multimerization; Dox, doxycycline; EGFP, enhanced GFP; EGF-R, epidermal growth factor receptor; EMT, epithelial-mesenchymal transition; FRET, fluorescence resonance energy transfer; GEF, guanine nucleotide exchange factor; MAP, microtubule-associated protein; MARK, microtubule affinity-regulating kinase; MDCK, Madin-Darby canine kidney; MKI, MARK kinase inhibitor sequence; PAR1, Partitioning-defective 1; PR, phosphorylation resistant; ROCK, RhoA-associated kinase.

Infection with *Helicobacter pylori cagA*-positive strains is the strongest risk factor for the development of gastric carcinoma, the second leading cause of cancer-related death worldwide (Peek and Blaser, 2002; Parkin, 2004; Hatakeyama, 2008). The *cagA* gene encodes an ~130–145-kD CagA protein, which is delivered via a bacterial type IV secretion system into gastric epithelial cells (Segal et al., 1999; Asahi et al., 2000; Backert et al., 2000; Odenbreit et al., 2000; Stein et al., 2000). Upon delivery, CagA is localized to the inner surface of the plasma membrane, where it undergoes tyrosine phosphorylation at the C-terminal Glu-Pro-Ile-Tyr-Ala (EPIYA) motifs by host cell kinases (Backert and Selbach, 2005). Tyrosine-phosphorylated CagA acquires the ability to specifically bind to and deregulate SH2 domain–containing proteins such as SHP-2, Csk, and Crk (Higashi et al., 2002; Tsutsumi et al., 2003; Suzuki et al., 2005). CagA also interacts with Grb2 and c-Met in a phosphorylation-independent manner (Mimuro et al., 2002; Churin et al., 2003). Accordingly, the bacterial oncoprotein mimics the function of mammalian scaffolding/adaptor proteins, such as Gab, and thereby manipulates host-signaling molecules to provoke pathogenic actions (Hatakeyama, 2008). Many, if not all, of these CagA–host protein interactions trigger a cascade of signaling events that culminate in activation of the Erk microtubule-associated protein (MAP) kinase pathway, deregulation of which generates a growth-promoting oncogenic signal, in both Ras-dependent and -independent manners (Mimuro et al., 2002; Churin et al., 2003; Higashi et al., 2004; Suzuki et al., 2005).

In polarized epithelial cells, CagA disrupts the tight junctions and causes loss of apical-basal epithelial polarity (Amieva et al., 2003; Saadat et al., 2007). This CagA activity is achieved through the interaction of CagA with Partitioning-defective 1 (PAR1)/microtubule affinity-regulating kinase (MARK), an evolutionally conserved serine/threonine kinase originally isolated in *Caenorhabditis elegans* which plays a fundamental role in the establishment and maintenance of cell polarity (Saadat et al., 2007; Zeaiter et al., 2008). In mammals, there are four PAR1 isoforms (PAR1a/MARK3, PAR1b/MARK2, PAR1c/MARK1,

Supplemental material can be found at:
http://doi.org/10.1084/jem.20100602

The Rockefeller University Press $30.00
J. Exp. Med. Vol. 207 No. 10 2157-2174
www.jem.org/cgi/doi/10.1084/jem.20100602

and PAR1d/MARK4) that redundantly phosphorylate MAPs and thereby destabilize microtubules, allowing asymmetric distribution of molecules which regulate cell polarity (Suzuki and Ohno, 2006). CagA functions as a universal inhibitor of PAR1 isoforms by directly binding to their kinase catalytic domains independent of CagA tyrosine phosphorylation (Saadat et al., 2007; Lu et al., 2009). The C-terminal 16-aa sequence of CagA that is specifically required for PAR1 binding has been designated as the CagA-multimerization (CM) sequence (Ren et al., 2006; Saadat et al., 2007; Lu et al., 2008). Recent structural analysis confirmed the importance of CM, which is also termed MARK kinase inhibitor sequence (MKI), for PAR1 interaction (Nesić et al., 2010).

Consistent with the tumor-relevant activities of CagA, proliferation of gastric epithelial cells in patients infected with *H. pylori cagA*-positive strains has been reported to be significantly higher than that in patients infected by *cagA*-negative strains (Peek et al., 1997; Cabral et al., 2007). Furthermore, systemic expression of CagA in mice led to the development of gastrointestinal and hematological malignancies (Ohnishi et al., 2008; Miura et al., 2009). Hence, CagA is the first bacterial oncoprotein to be discovered in the context of human malignancy. Paradoxically, however, CagA has also been reported to act as a potent inhibitor of cell proliferation in vitro, an observation which is inconsistent with the oncogenic role of CagA (Tsutsumi et al., 2003; Higashi et al., 2004; Murata-Kamiya et al., 2007).

In this paper, we show that CagA-deregulated Erk signaling in nonpolarized epithelial cells induces accumulation of the $p21^{Waf1/Cip1}$ cyclin-dependent kinase (CDK) inhibitor (hereafter referred to as p21), which in turn causes senescence-like proliferation arrest. In contrast, deregulated Erk signaling caused by CagA in polarized epithelial cells induces proliferation without accumulation of p21. We then describe the mechanism that determines the fate of epithelial cells in response to CagA, either senescence or forced mitogenesis, in an epithelial polarity-dependent manner. Our work reveals that CagA exploits the guanine nucleotide exchange factor (GEF)–H1–RhoA–RhoA-associated kinase (ROCK)–c-Myc–microRNA–p21 axis, a long-sought signaling pathway which connects epithelial polarity with the cell cycle, to exert its oncogenic action.

RESULTS

Expression of CagA in nonpolarized epithelial cells induces cellular senescence

To investigate the effect of *H. pylori* CagA on epithelial cell proliferation, we inducibly expressed CagA in MKN28 human gastric epithelial cells using a tet-off system. As previously reported, CagA activated Erk MAP kinase but paradoxically inhibited cell proliferation, which was concomitantly associated with the accumulation of the CDK inhibitor p21 in cells (Fig. 1, A and B; Tsutsumi et al., 2003; Higashi et al., 2004; Murata-Kamiya et al., 2007). The growth-inhibitory activity of CagA was reproduced in AGS human gastric epithelial cells (Fig. S1, A and B). Knockdown of p21 by specific short hairpin (sh) RNA or small interfering (si) RNA abolished the ability of CagA to inhibit cell proliferation, indicating that elevated p21 was responsible for the CagA-mediated proliferation arrest (Fig. 1 C and Fig. S1 C). Treatment of cells with a MEK inhibitor U0126 also abrogated p21 accumulation by CagA (Fig. 1 D), whereas inhibition of PKC, PI-3 kinase, or PLC-γ, each of which can independently induce p21, did not have any effect on the CagA-mediated p21 accumulation (not depicted). Thus, CagA causes accumulation of p21 through Erk signaling. After exposure to CagA for 5 d, proliferation-arrested cells became flat and expressed senescence-associated β-galactosidase (Fig. 1 E). These results indicated that CagA expressed in nonpolarized epithelial cells aberrantly activates Erk signaling, which induces the accumulation of p21 and thereby causes senescence-like proliferation arrest.

Expression of CagA in polarized epithelial cells elicits forced mitogenesis

The observations described in the previous section, in turn, indicated that CagA must have a mechanism that converts the response of host epithelial cells from growth inhibition to growth stimulation to exert its oncogenic action. During *H. pylori* infection in the stomach, CagA is delivered into the gastric mucosal monolayer comprised of epithelial cells with highly developed apical-basal polarity. We therefore sought to determine the effect of CagA on polarized epithelial cells, pathophysiologically relevant target cells for *H. pylori*. To this end, we used the Madin-Darby canine kidney (MDCK) II model epithelial monolayer. To prepare a polarized epithelial monolayer, we cultured MDCK cells on Transwell membrane filters for 3 d. In all experiments using polarized MDCK cells described in this paper, the establishment of apical-basal epithelial polarity was confirmed by staining cells with the tight junction marker ZO-1 (Fig. S2, representative staining images of polarized MDCK monolayers).

As previously described, expression of CagA in polarized MDCK cells led to the dissolution of tight junctions and loss of apical-basal polarity, followed by extrusion of CagA-expressing cells from the polarized monolayer (Amieva et al., 2003; Saadat et al., 2007). To our surprise, CagA-expressing cells that had extruded from the monolayer underwent multiple rounds of cell divisions without showing p21 accumulation (Fig. 2, A and B). Both WT CagA and phosphorylation-resistant (PR) CagA were capable of inducing DNA synthesis when expressed in polarized epithelial cells, although the degree of DNA synthesis induced by PR CagA was weaker than that induced by WT CagA (Fig. 2 C). To determine whether the observed mitogenesis by CagA is cell polarity dependent or cell type dependent, we transiently expressed CagA in nonpolarized MDCK cells, which had been prepared by plating MDCK cells in a standard cell culture condition without using Transwell and found that, as in MKN28 and AGS cells, CagA induced p21 and inhibited cell proliferation independently of cell density (Fig. S3). The possibility that the Transwell culture on its own modified cellular response to CagA was excluded from the observation that expression of CagA in Transwell-cultured

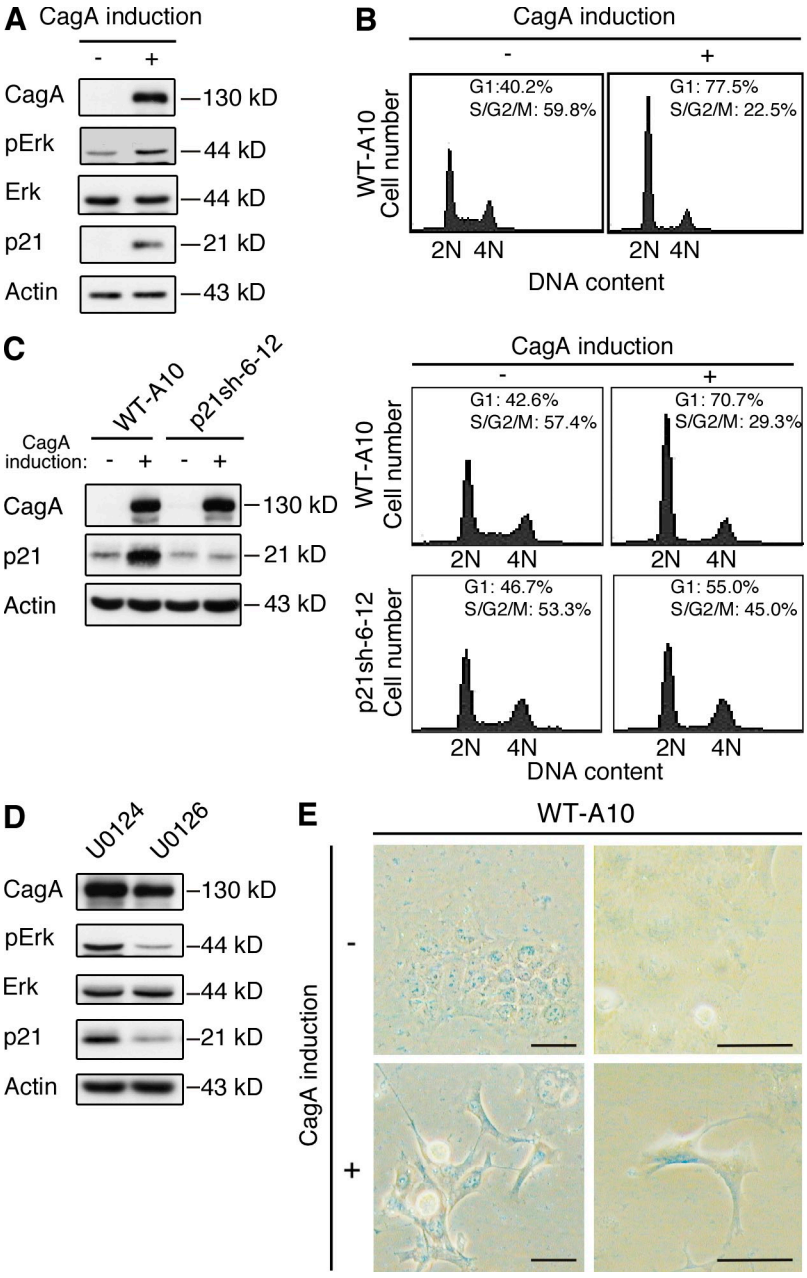

Figure 1. Growth inhibition of nonpolarized epithelial cells by CagA. (A) MKN28-derived WT-A10 cells that inducibly express HA-tagged CagA by tet-off system were cultured in the presence or absence of 0.2 µg/ml doxycycline (Dox). Cell lysates were subjected to immunoblotting with the indicated antibodies. (B) WT-A10 cells were cultured in the presence or absence of Dox. Cells were stained with propidium iodide and were subjected to cell cycle analysis using flow cytometry. Percentages of cells in G1 and S/G2/M phases are shown. Results were reproducible in three independent experiments. (C, left) WT-A10 cells and WT-A10–derived p21sh-6-12 cells, in which p21 was knocked down by specific siRNA, were induced to express CagA by depleting Dox from the culture for 24 h. Cell lysates were subjected to immunoblotting with anti-HA, anti-p21, and anti-actin antibodies. (C, right) Cells were stained with propidium iodide and were subjected to flow cytometric analysis. Percentages of cells in G1 and S/G2/M phases are shown. (D) WT-A10 cells expressing CagA were treated with 25 µM MEK inhibitor U0126 or control U0124. Cell lysates were subjected to immunoblotting. (E) WT-A10 cells were cultured for 5 d in the presence or absence of Dox to induce CagA expression, and senescence-associated β-galactosidase activity was visualized by staining cells with X-Gal (blue). Light micrograph images are shown. Bars, 100 µm. Representative gel (A, C, and D) and staining (E) images obtained from three independent experiments are shown.

MKN28 cells, which cannot develop tight junctions and apical-basal epithelial polarity, induced p21 (Fig. S4). In contrast to WT CagA, CagA-ΔCM/MKI, which does not bind PAR1 and thus cannot disrupt epithelial polarity, failed to provoke cell extrusion and subsequent mitogenesis when expressed in polarized MDCK cells (Fig. 2 C). Accordingly, the mitogenic effect of CagA is epithelial-polarity context dependent. Treatment of polarized MDCK cells with U0126 abolished extrusion of CagA-expressing cells from the polarized monolayer and subsequent mitogenesis, indicating that, like PAR1 inhibition, CagA-induced Erk activation is required for both extrusion and proliferation (Fig. 2 D). We also investigated the polarity-dependent effects of CagA on cell proliferation using MDCK cells that inducibly express WT CagA (MDCK-WT-CagA cells) or PR CagA (MDCK-PR-CagA cells) by a tet-on system (Fig. S5). As expected, induction of CagA in nonpolarized MDCK cells caused p21-mediated cell senescence, whereas CagA, either WT or phosphorylation-resistant mutant, inducibly expressed in polarized epithelial cells initiated DNA synthesis (Fig. S5). Collectively, these observations indicated that aberrant Erk signaling, which is activated via both tyrosine phosphorylation-dependent and -independent CagA activities, can induce opposite cellular responses, senescence, and forced mitogenesis, depending on the polarity status of the epithelial cell to which CagA is delivered.

It has been reported that CagA and the vacuolating toxin VacA, another *H. pylori* virulence factor, down-regulate each other's effects on epithelial cells (Yokoyama et al., 2005; Argent et al., 2008; Tegtmeyer et al., 2009). In particular, VacA has been shown to inhibit Erk signaling by inactivating epidermal growth factor receptor (EGF-R) and HER2/neu kinases, although the underlying mechanisms remain unknown (Tegtmeyer et al., 2009). To investigate whether VacA influences the polarity context-dependent action of CagA on cell proliferation, we expressed CagA in polarized or nonpolarized MDCK cells in the presence or absence of 5 µg/ml of acid-activated VacA. The VacA treatment potently induced vacuolation of MDCK cells but did not influence the polarity-dependent regulation of p21 by CagA (Fig. 2, E–G). These observations argue against

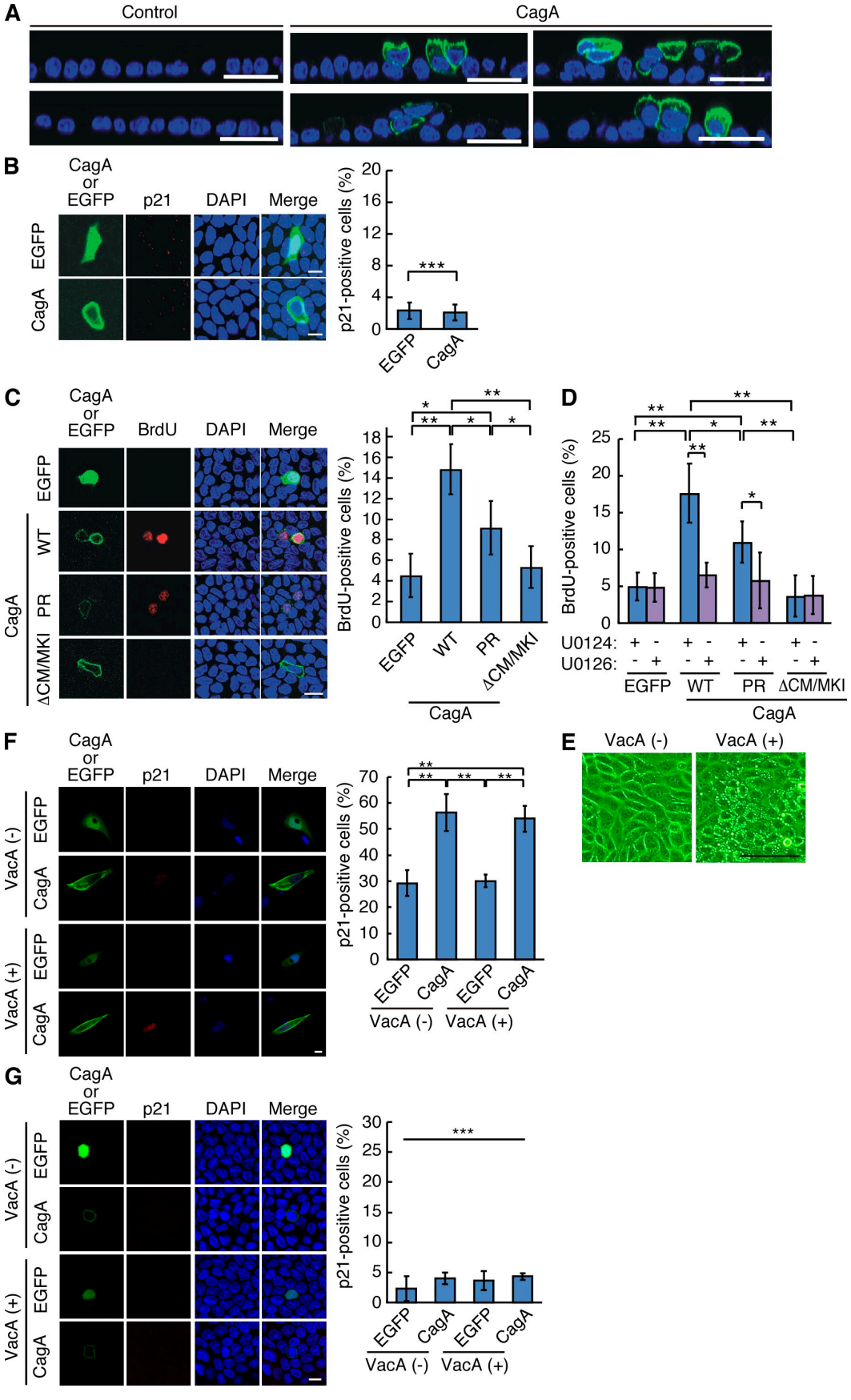

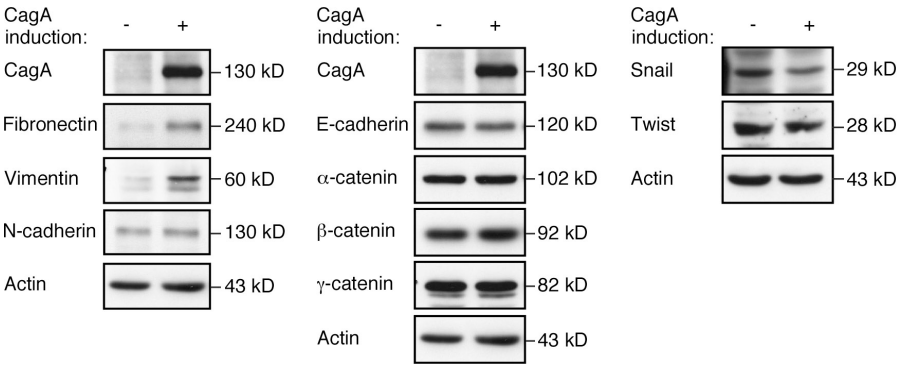

Figure 3. Induction of mesenchymal markers in epithelial cells expressing CagA. MDCK-WT-CagA cells were induced to express CagA by culturing them in medium containing Dox for 48 h. Cell lysates were immunoblotted with antibodies specific for mesenchymal markers (left), epithelial markers (middle), and EMT-regulating transcription factors (right). Three independent blots yielded similar results.

the idea that VacA directly modulates the effect of CagA on proliferation of both polarized and nonpolarized MDCK epithelial cells. Because infection of polarized MDCK cells with *H. pylori* was extremely difficult (unpublished data), we could not investigate the polarity-dependent effect of VacA on CagA by infection experiments with MDCK cells.

CagA-induced mitogenesis is associated with epithelial–mesenchymal transition (EMT)

Extrusion of CagA-expressing cells from the polarized epithelial monolayer was concomitantly associated with the morphological transition of epithelial cells from a polarized state to an invasive phenotype, a cellular change characteristic of EMT (Fig. 2 A; Bagnoli et al., 2005). To investigate CagA-induced EMT in more detail, we examined the expression of mesenchymal markers after expression of CagA in MDCK cells and found that CagA significantly increased levels of mesenchymal proteins such as vimentin and fibronectin (Fig. 3, left). However, CagA expression did not down-regulate epithelial markers such as E-cadherin, α-catenin, β-catenin, and γ-catenin (Fig. 3, middle). Furthermore, there was no up-regulation of EMT-inducing transcription factors, such as Twist and Snail, in cells expressing CagA (Fig. 3, right). Hence, CagA-expressing cells that have undergone morphological EMT simultaneously express both epithelial and mesenchymal markers.

RhoA suppresses CagA-induced p21 accumulation

We next investigated the mechanism by which CagA-dependent p21 accumulation is abolished in an epithelial-polarity context-dependent manner. It has been reported that RhoA counteracts induction of p21 by oncogenic Ras signaling (Adnane et al., 1998; Olson et al., 1998; Sahai et al., 2001; Liberto et al., 2002; Coleman et al., 2006). We therefore postulated that RhoA is involved in the inhibition of CagA-dependent p21 accumulation. To test this idea, we treated polarized MDCK cells with a membrane-permeable RhoA inhibitor, *Clostridium botulinum* C3 transferase. The C3 transferase treatment caused accumulation of p21 in polarized epithelial cells expressing CagA (Fig. 4, A and B). Furthermore, RhoA was activated upon expression of CagA in polarized epithelial cells but not in nonpolarized epithelial cells, as determined by a GST pull-down assay (Fig. 4, C and D) or the use of a RhoA-specific fluorescence resonance energy transfer (FRET) probe (Fig. 4 E). From these observations, we concluded that activation of RhoA overcomes CagA/Erk-dependent accumulation of p21.

GEF-H1 mediates CagA-dependent RhoA activation in polarized epithelial cells

The observations described in the previous section prompted us to investigate the mechanism underlying RhoA activation by CagA. RhoA activity is controlled via the interplay between activators, GEFs, and inhibitors, GAPs (GTPase-activation

Figure 2. Induction of forced mitogenesis upon expression of CagA in polarized epithelial cells. (A) After expression of HA-tagged CagA in polarized MDCK cells, CagA-positive cells were visualized with anti-HA antibody (green). Polarized MDCK cells without CagA expression were used as a control. Nuclei in confocal x-z images were visualized by 4,6-diamidino-2-phenylindole (DAPI) staining (blue). Bars, 10 µm. (B, left) Polarized MDCK cells transfected with an HA-tagged CagA vector were stained with anti-HA antibody (green), anti-p21 antibody (red), and DAPI (blue). Confocal x-y images are shown. Bars, 10 µm. (B, right) Percentage of p21-positive cells in cells expressing CagA or EGFP. Error bars indicate mean ± SD. $n = 3$. ***, $P > 0.05$. (C, left) Confocal x-y images of polarized MDCK cells transfected with an expression vector encoding HA-tagged CagA (WT, PR, and ΔCM/MKI, CagA lacking the PAR1/MARK-binding sequence) were stained with anti-HA antibody (green), anti-BrdU antibody (red), and DAPI (blue). An expression vector for enhanced GFP (EGFP) was used as a control. Bar, 10 µm. (C, right) Percentage of BrdU-positive cells in cells expressing CagA or EGFP. Error bars indicate mean ± SD. $n = 5$. **, $P < 0.01$; *, $P < 0.05$. (D) Percentage of BrdU-positive cells in polarized MDCK cells expressing CagA or EGFP in the presence of a specific MEK inhibitor U0126 or its inactive analogue U0124 at a final concentration of 25 µM. Error bars indicate mean ± SD. $n = 5$. **, $P < 0.01$; *, $P < 0.05$. (E) Induction of vacuolation of MDCK cells by VacA treatment. Light micrograph images are shown of MDCK cells treated with 5 µg/ml of acid-activated VacA for 54 h. Bar, 100 µm. (F and G, left) Confocal x-y images of nonpolarized (F) and polarized (G) MDCK cells expressing EGFP or CagA in the presence or absence of 5 µg/ml of acid-activated VacA. Bar, 10 µm. (F and G, right) Percentage of p21-positive cells among cells expressing EGFP or CagA in the presence or absence of acid-activated VacA. Error bars indicate mean ± SD. $n = 3$. **, $P < 0.01$; ***, $P > 0.05$. Representative images from three independent experiments are shown in all panels.

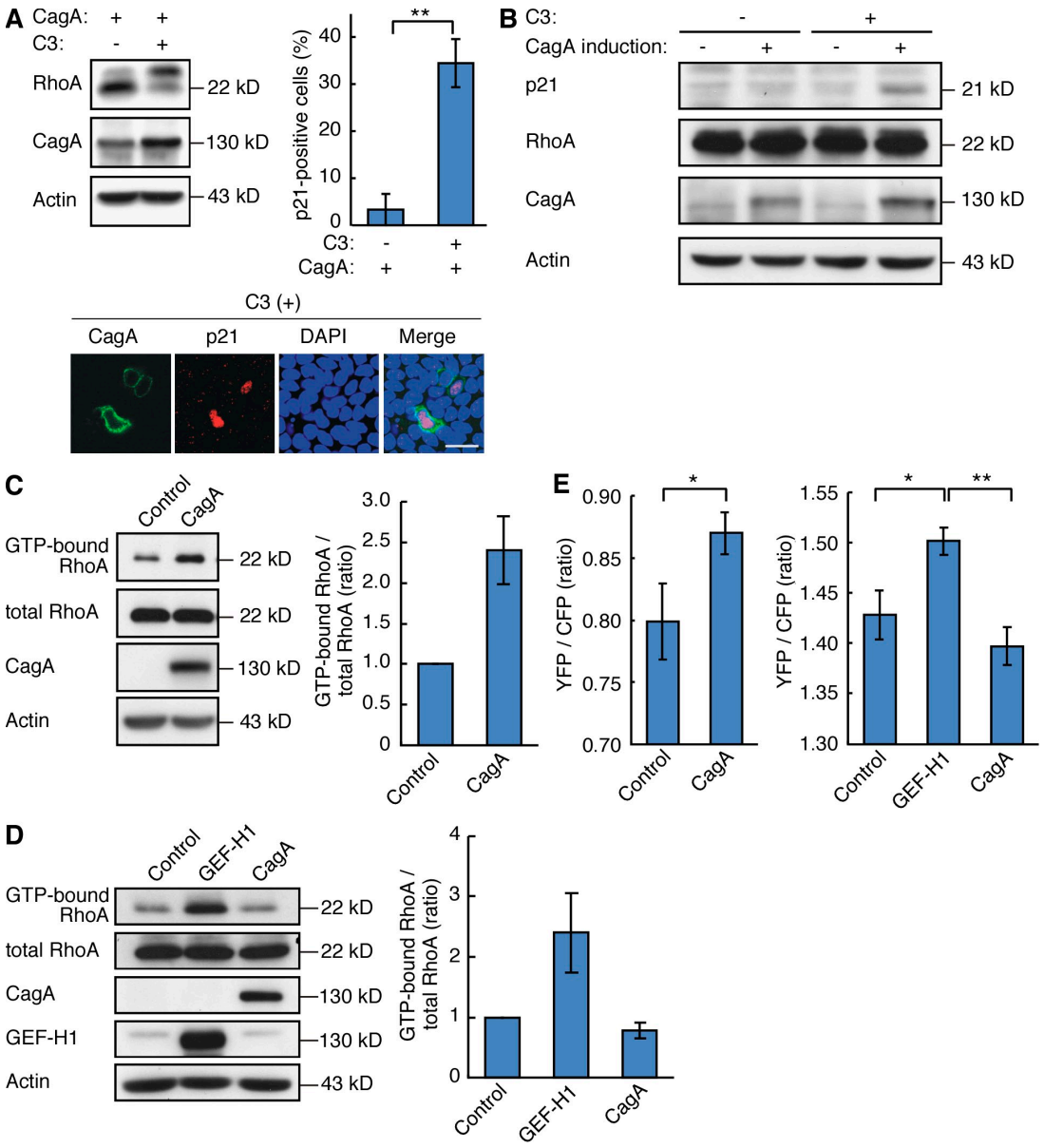

Figure 4. CagA expressed in polarized epithelial cells inhibits p21 accumulation via RhoA. (A, top left) Polarized MDCK cells were transfected with an expression vector for HA-tagged CagA in the presence or absence of C3 transferase, an inhibitor of RhoA. Cell lysates were immunoblotted with the indicated antibodies. (A, top right) Percentage of p21-positive cells in cells expressing CagA in the presence or absence of C3. Error bars indicate mean ± SD. $n = 3$. **, $P < 0.01$. (A, bottom) Confocal x-y images of cells stained with anti-p21 antibody (red), anti-HA antibody (green), and DAPI (blue). Bar, 10 µm. (B) CagA-inducible MDCK-WT-CagA cells were polarized by Transwell filter culture for 3 d. Cells were then cultured in the absence (CagA noninduced) or presence (CagA induced) of Dox with or without 5 µg/ml of membrane-permeable C3 transferase. After 15 h, cell lysates were prepared and subjected to immunoblotting with the indicated antibodies. (C, left) RhoA activity was measured by a GST-RBD-Rhotekin pulldown assay in polarized MDCK cells infected with adenovirus transducing CagA or β-galactosidase (control). (C, right) GTP-bound RhoA/total RhoA ratio. Error bars indicate mean ± SD. $n = 3$. (D, left) RhoA activity was measured by a GST-RBD-Rhotekin pulldown assay in nonpolarized MDCK cells transfected with a CagA, GEF-H1, or control empty vector. (D, right) GTP-bound RhoA/total RhoA ratio. Error bars indicate mean ± SD. $n = 3$. (E, left) Polarized MDCK cells were coinfected with recombinant adenoviruses encoding a RhoA-FRET probe and CagA. (E, right) Nonpolarized MDCK cells were transfected with an expression vector for CagA or GEF-H1 together with the pRaichu-RhoA reporter plasmid encoding a RhoA probe with the configuration of YFP-RhoA–binding domain of the effector (protein kinase PKN) RhoA-CFP. Cells were harvested and YFP/CFP emission ratio (530/475 nm) was calculated. Error bars indicate mean ± SD. $n = 3$. **, $P < 0.01$; *, $P < 0.05$. Representative gel (A–D) and staining images (A) from three independent experiments are shown.

proteins). Among various RhoA-specific GEFs, GEF-H1 was of particular interest because the GEF activity is regulated by polarity-dependent mechanisms (Birkenfeld et al., 2008). In nonpolarized MDCK cells, GEF-H1 was distributed to the cytoplasm, where it was associated with microtubules (Fig. 5 A). This GEF-H1–microtubules interaction has

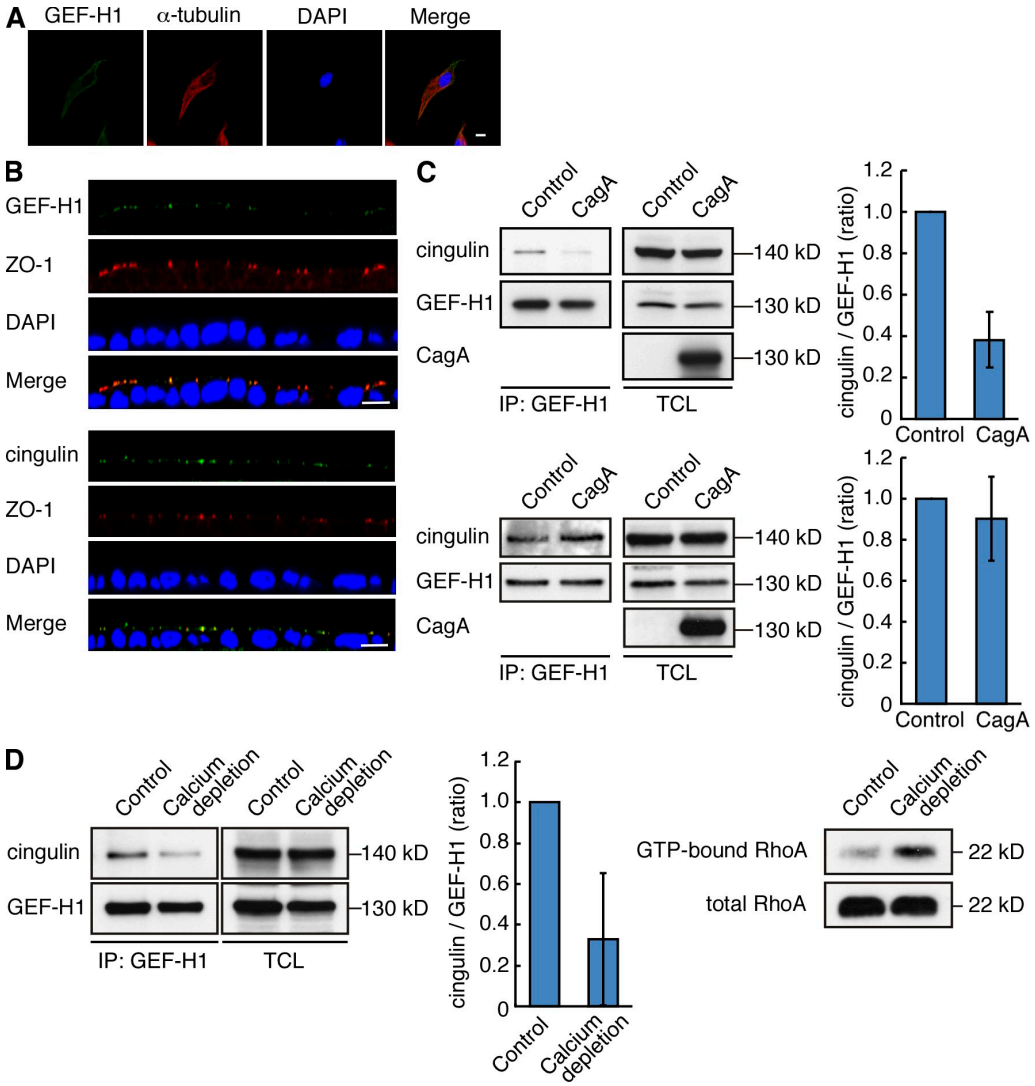

Figure 5. Activation of RhoA by disruption of the GEF-H1–cingulin complex. (A) Confocal x-y images of GEF-H1 and microtubules in nonpolarized MDCK cells. Cells were stained with anti–GEF-H1 antibody (green), anti–α-tubulin antibody (red), and DAPI (blue). Bar, 10 µm. (B) Confocal x-z images of GEF-H1 and cingulin in polarized MDCK cells. Cells were stained with anti–GEF-H1 antibody (green, top), anti-cingulin antibody (green, bottom), anti–ZO-1 antibody (red), and DAPI (blue). Bars, 10 µm. (C, left) Polarized (top) or nonpolarized (bottom) MDCK cells were infected with adenovirus encoding CagA or β-galactosidase (control). Total cell lysates were immunoprecipitated with an anti–GEF-H1 antibody and were subjected to immunoblotting with the indicated antibodies. (C, right) Quantitation of GEF-H1-bound cingulin. Error bars indicate mean ± SD. $n = 3$. (D, left) Polarized MDCK cells were cultured in calcium-free medium (calcium depletion) or normal medium (control) for 24 h. Total cell lysates were immunoprecipitated with an anti–GEF-H1 antibody and were subjected to immunoblotting with the indicated antibodies. (D, middle) Quantitation of GEF-H1–bound cingulin. Error bars indicate mean ± SD. $n = 3$. (D, right) RhoA activity was measured by a GST-RBD-Rhotekin pulldown assay in polarized MDCK cells or MDCK cells depolarized by calcium depletion. Representative staining (A and B) and gel (C and D) images from three independent experiments are shown.

been reported to inhibit RhoA-specific GEF activity of GEF-H1 (Krendel et al., 2002; Birkenfeld et al., 2008; Chang et al., 2008). In polarized MDCK cells, however, GEF-H1 was translocalized to the membrane and was concentrated to the tight junctions. At the tight junctions, GEF-H1 specifically interacted with a GEF-H1 inhibitor, cingulin, as previously reported (Fig. 5 B; Aijaz et al., 2005; Birkenfeld et al., 2008). Accordingly, we investigated the effect of CagA on the level of GEF-H1–cingulin complex in polarized epithelial cells. To this end, we immunoprecipitated GEF-H1 in lysates prepared from polarized MDCK cells with or without CagA expression and then immunoblotted the GEF-H1 immunoprecipitates with an anti-cingulin antibody. As shown in Fig. 5 C (top), the amount of GEF-H1-bound cingulin was markedly decreased when CagA was coexpressed in polarized MDCK cells. In contrast, there was no change in the amount of GEF-H1–bound cingulin by CagA in nonpolarized MDCK cells (Fig. 5 C, bottom). The observations indicated that, upon expression in polarized epithelial cells, CagA disrupts the GEF-H1–cingulin complex and, thereby, liberates

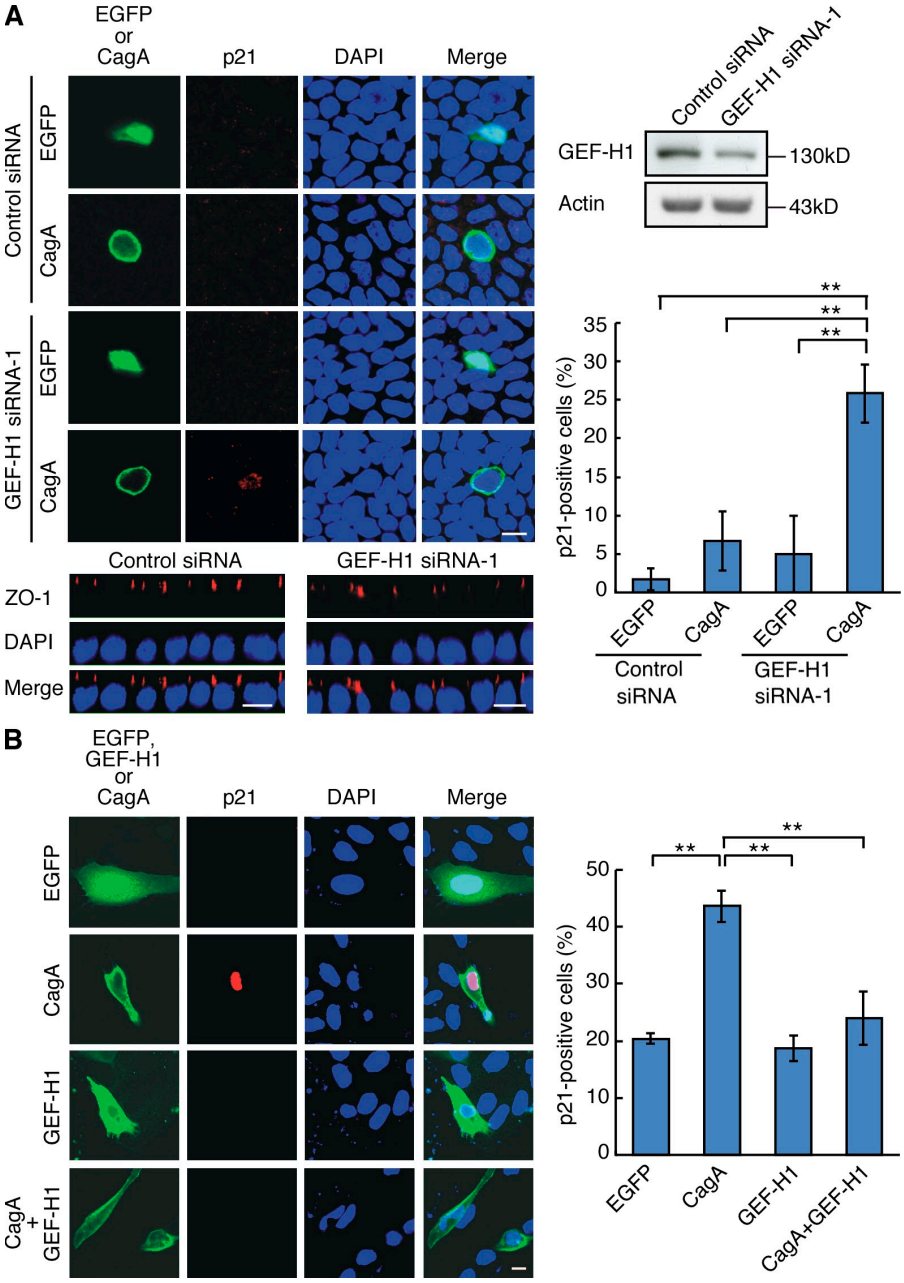

Figure 6. Requirement of GEF-H1 for the inhibition of CagA-mediated p21 accumulation in polarized epithelial cells. (A, left) Polarized MDCK cells treated with 100 pmol GEF-H1 siRNA-1 or firefly luciferase–specific siRNA (control siRNA) were transfected with CagA or EGFP expression vector. Cells were stained with anti-p21 antibody (red, top, confocal x-y view) or anti–ZO-1 antibody (bottom, confocal x-z view). Bars, 10 µm. (A, right) Cell lysates were subjected to immunoblotting (top). Percentage of p21-positive cells in GEF-H1 knockdown MDCK cells expressing CagA or EGFP. Error bars indicate mean ± SD. $n = 3$. **, $P < 0.01$ (bottom). (B, left) Nonpolarized MDCK cells transfected with CagA and/or GEF-H1 vector were stained with anti-p21 antibody (red, confocal x-y view). Bar, 10 µm. (B, right) Percentage of p21-positive cells in MDCK cells expressing EGFP, CagA, GEF-H1, or CagA plus GEF-H1. Error bars indicate mean ± SD. $n = 3$. **, $P < 0.01$. Representative staining images from three independent experiments are shown.

GEF-H1 from the constraints by cingulin. To investigate whether junctional and polarity defects caused by CagA are responsible for disruption of the GEF-H1–cingulin complex, we destroyed the apical junctional complex of polarized MDCK cells by calcium depletion. Like CagA, calcium depletion led to dissociation of cingulin from GEF-H1, which was concomitantly associated with RhoA activation as determined by a pulldown assay (Fig. 5 D). These results indicated that junctional and polarity defects, whether they are induced by CagA or calcium depletion, cause disruption of the GEF-H1–cingulin complex and subsequent activation of GEF-H1 and then RhoA.

To consolidate the importance of GEF-H1 in the suppression of p21 expression, we inhibited GEF-H1 expression by specific siRNA in polarized MDCK cells and found that the GEF-H1 knockdown led to the accumulation of p21 in cells expressing CagA (Fig. 6 A and Fig. S6). Conversely, coexpression of GEF-H1 with CagA in nonpolarized MDCK cells abolished CagA-mediated p21 accumulation (Fig. 6 B). From these observations, we concluded that specific activation of GEF-H1 by CagA expressed in polarized epithelial cells stimulates RhoA, which in turn suppresses p21 accumulation.

Sustained membrane localization of GEF-H1 upon expression of CagA in polarized epithelial cells

We next wished to gain an insight into the mechanism by which CagA expressed in polarized epithelial cells enforces mitogenesis even after cells become nonpolarized. As described in the previous section, expression of CagA under a polarized condition activates GEF-H1, whereas CagA expression in a nonpolarized condition fails to do so. Because GEF-H1–mediated RhoA activation is required for the suppression of p21 accumulation, there must be a mechanism that keeps GEF-H1 in its active form when CagA was introduced into polarized epithelial cells. In this regard, GEF-H1 has been reported to bind PAR1d, a member of the PAR1/MARK family (Brajenovic et al., 2004). We confirmed and extended the observation by showing that all of the PAR1 isoforms (PAR1a-d) interact with GEF-H1 independent of cingulin binding (Fig. 7 A). Because CagA also binds to these PAR1 isoforms (Saadat et al., 2007; Lu et al., 2009),

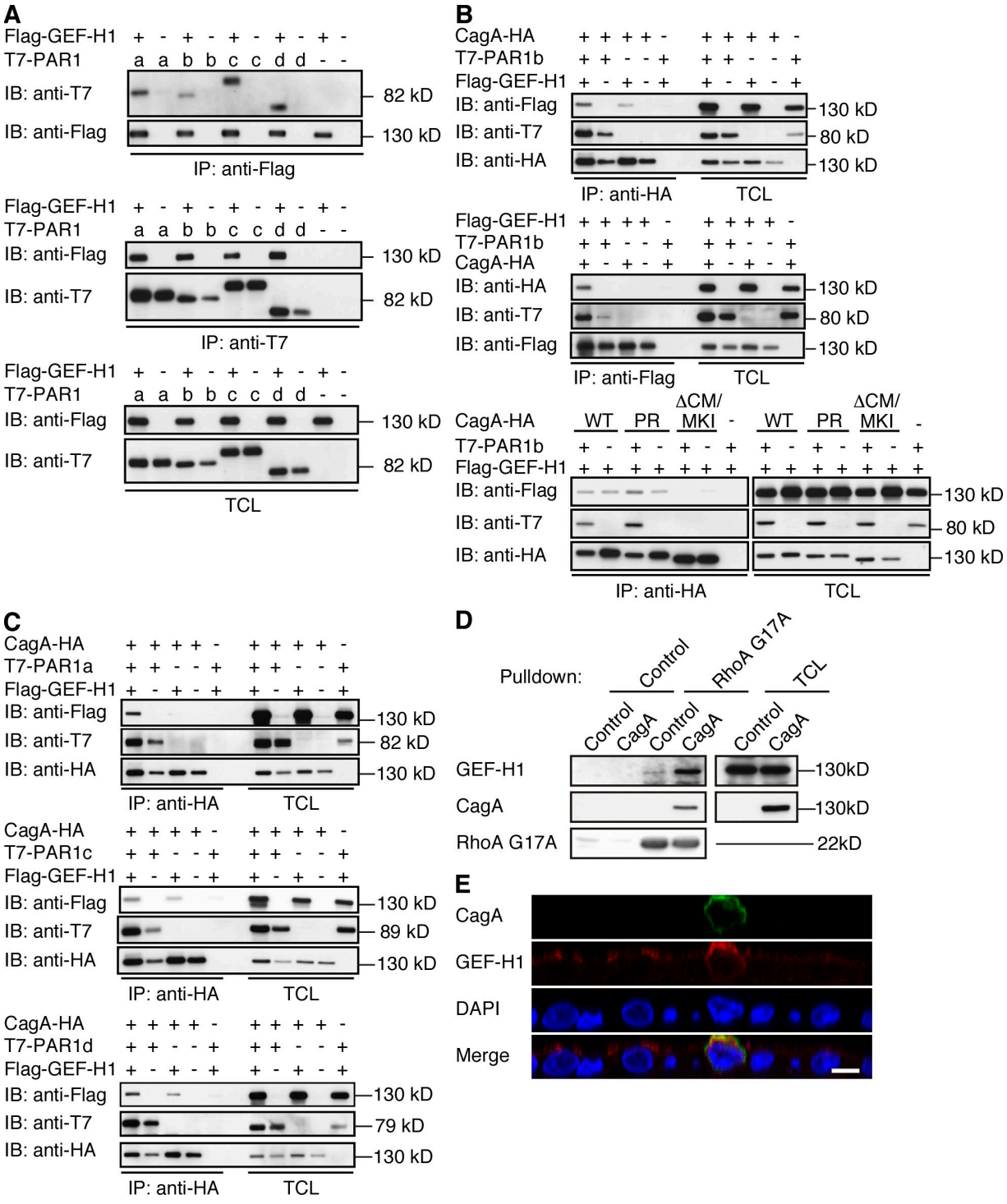

Figure 7. Complex formation of CagA, PAR1, and GEF-H1 (A) COS-7 cells were transfected with T7-tagged PAR1 (PAR1a, PAR1b, PAR1c, or PAR1d) and/or Flag-tagged GEF-H1 vector. Total cell lysates were immunoprecipitated with anti-HA or anti-Flag antibody and immunoblotted with indicated antibodies. (B) COS-7 cells were transfected with indicated vectors. Total cell lysates were immunoprecipitated with anti-HA or anti-Flag antibody and immunoblotted with indicated antibodies. (C) COS-7 cells were transfected with indicated vectors. Total cell lysates were immunoprecipitated with anti-HA antibody and immunoblotted with indicated antibodies. (D) Polarized MDCK cells were infected with an adenovirus transducing CagA or β-galactosidase (control). Total cell lysates were pulled down with RhoA G17A (nucleotide-free RhoA) beads and were subjected to immunoblotting with the indicated antibodies. (E) Polarized MDCK cells were transfected with a CagA expression vector. At 27 h after transfection, cells were fixed and stained with anti-HA antibody (green), anti-GEF-H1 antibody (red), and DAPI (blue). Shown are x-z confocal images. Bar, 10 µm. Representative gel (A–D) and staining (E) images from three independent experiments are shown.

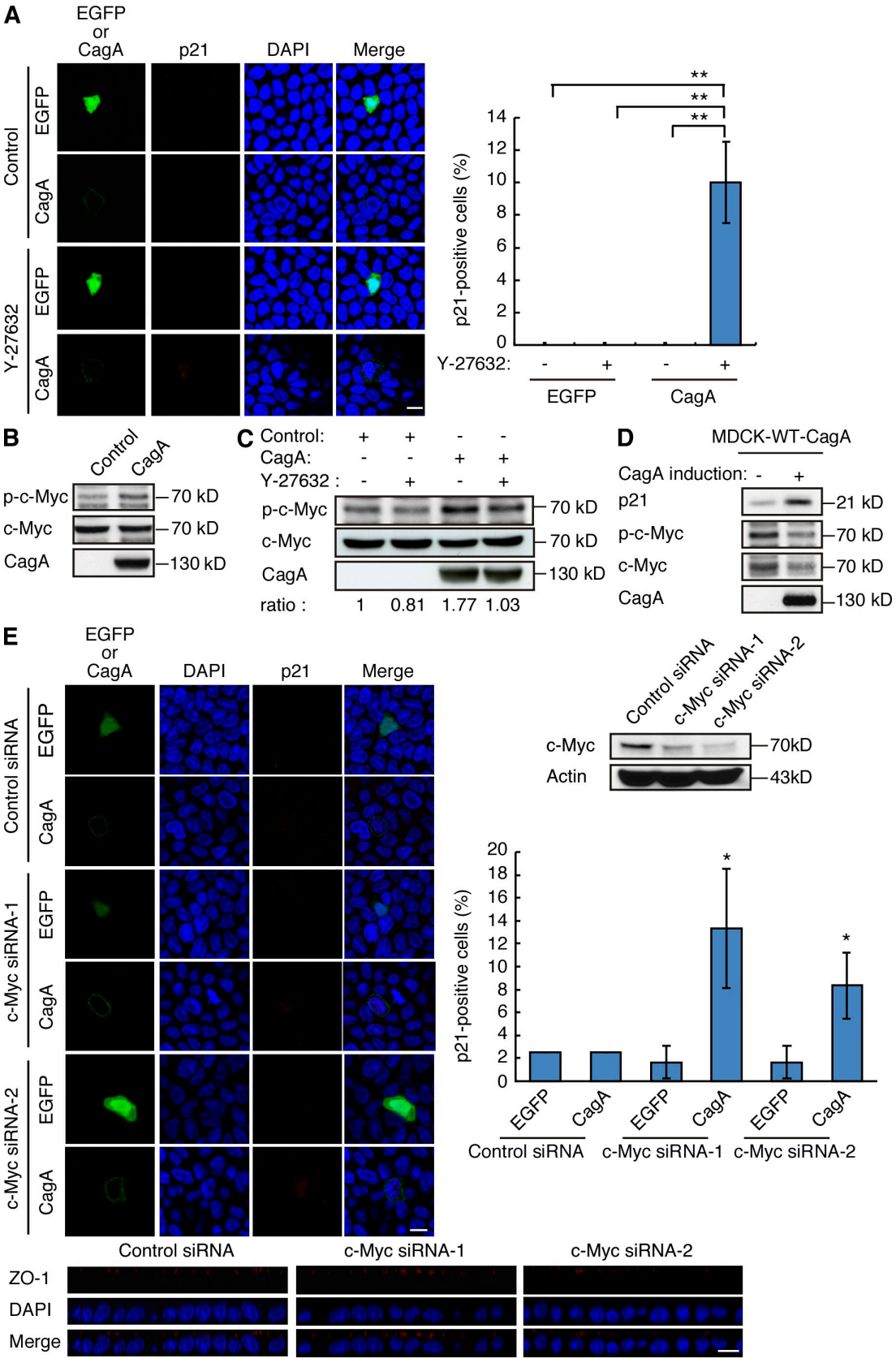

we hypothesized that CagA can associate with GEF-H1 using PAR1 as an adaptor. Upon triple transfection in COS-7 cells, we found that CagA forms a physical complex with GEF-H1 via PAR1 (Fig. 7, B and C). We also found that RhoA G17A, which specifically binds to the active form of GEF-H1 (García-Mata et al., 2006), pulled down GEF-H1 together with CagA, indicating that GEF-H1 was active in the heterotrimeric complex (Fig. 7 D). Because CagA is tethered to the plasma membrane, the CagA–PAR1–GEF-H1 heterotrimeric complex should prevent translocation of GEF-H1 to the cytoplasm, where it becomes inactivated. Consistent with this notion, GEF-H1 was colocalized with CagA at the membrane in CagA-expressing cells that had been expelled from the polarized monolayer (Fig. 7 E). These results indicate that sustained membrane localization of active GEF-H1 by CagA enables continued RhoA activation, which inhibits p21 accumulation, during and after transition of epithelial cells from a polarized state to nonpolarized state.

Downstream effectors of RhoA that inhibit p21 accumulation

RhoA has two well known downstream effectors: Rho-associated kinase (ROCK) and formin homology protein mDia. To further delineate the mechanism by which active RhoA inhibits CagA-dependent p21 accumulation, we examined the effect of Y-27632, a specific inhibitor of ROCK. Treatment of polarized MDCK cells with Y-27632 led to the CagA-dependent accumulation of p21, indicating that ROCK is the downstream effector of RhoA that mediates p21 suppression (Fig. 8 A). We next investigated the mechanism underlying ROCK-mediated suppression of p21 accumulation. Previous studies demonstrated that ROCK stimulates c-Myc, which has been reported to effectively inhibit p21 expression (Watnick et al., 2003; Liu et al., 2009b). Consistent with this, the level of phospho-c-Myc, the active form of c-Myc, was markedly increased upon expression of CagA in polarized MDCK cells (Fig. 8 B and Fig. S7 A). This increase in the active form of c-Myc was inhibited by Y-27632 (Fig. 8 C and Fig. S7 B). In contrast, expression of CagA in nonpolarized MDCK cells induced p21 accumulation but failed to activate c-Myc (Fig. 8 D). To consolidate the role of c-Myc in CagA-dependent inhibition of p21 accumulation, we specifically inhibited c-Myc expression by siRNA in polarized MDCK cells. We found that down-regulation of c-Myc causes accumulation of p21 in CagA-expressing MDCK cells (Fig. 8 E). These observations indicated that CagA expressed in polarized epithelial cells activates the GEF-H1–RhoA–ROCK cascade, which in turn stimulates c-Myc to repress CagA-dependent p21 accumulation.

It has been reported that RhoA-mediated inhibition of p21 accumulation involves posttranscriptional mechanisms (Coleman et al., 2006). Recently, microRNAs have emerged as key posttranscriptional regulators for gene expression (Bartel, 2004). Intriguingly, c-Myc has been shown to induce the miR-17-92 cluster, which contains miR-17 and miR-20a that target *p21* mRNA (Petrocca et al., 2008; Inomata et al., 2009). We therefore hypothesized that c-Myc–regulated miR-17-92 is involved in the regulation of p21 expression in cells expressing CagA. Quantitative RT-PCR analysis revealed that expression of CagA in polarized MDCK cells (Fig. 9 A) or depolarization of MDCK cells by calcium depletion (Fig. S7 C) elicits significant increases in the amounts of miR-17 and miR-20a, which were abolished by treatment of cells with the ROCK inhibitor Y-27632. Again, the presence of VacA did not influence induction of these microRNAs by CagA (Fig. 9 B). To consolidate the role of c-Myc in CagA-dependent elevation of the microRNAs, we specifically inhibited c-Myc expression by siRNA in polarized MDCK cells. We found that down-regulation of c-Myc abolishes induction of miR-17 or miR-20a by CagA (Fig. 9 C). Conversely, inhibition of miR-17 and miR-20a expression by antisense oligonucleotides in polarized epithelial cells led to the accumulation of p21 by CagA (Fig. 9 D). These observations indicated that c-Myc–induced miR-17 and/or miR-20a plays a dominant role in the inhibition of CagA-dependent p21 accumulation.

DISCUSSION

In the present study, we found that *H. pylori* CagA expressed in nonpolarized epithelial cells aberrantly activates growth-promoting Erk signaling, which exerts an oncogenic stress that gives rise to p21 accumulation and subsequent cellular senescence. In striking contrast, expression of CagA in polarized

Figure 8. Involvement of the ROCK–c-Myc pathway in the suppression of p21 upon expression of CagA in polarized epithelial cells. (A, left) Polarized MDCK cells were transfected with indicated vectors. At 6 h after transfection, cells were treated with 50 µM Y-27632 and were cultured for additional 21 h. Cells were then stained with anti-p21 antibody (red), anti-HA antibody (green), and DAPI (blue). Confocal x-y images are shown. Bar, 10 µm. (A, right) Percentage of p21-positive cells in MDCK cells expressing EGFP or CagA. Error bars indicate mean ± SD. $n = 3$. **, $P < 0.01$. (B) Polarized MDCK cells were infected with adenovirus transducing CagA or β-galactosidase (control) for 24 h. Cell lysates were immunoblotted with indicated antibodies. p-c-Myc, phospho-c-Myc. (C) Polarized MDCK cells were infected with adenovirus encoding CagA or β-galactosidase (control). At 6 h after infection, cells were treated with 50 µM Y-27632 and were cultured for an additional 18 h. Cell lysates were immunoblotted with the indicated antibodies. Phospho-c-Myc (p-c-Myc)/total c-Myc ratio (under blot) was obtained by quantitation of the corresponding protein bands using a luminescence image analyzer. (D) CagA-inducible MDCK-WT-CagA cells were cultured for 24 h in the presence or absence of Dox. Cell lysates were immunoblotted with indicated antibodies. (E, left) Polarized MDCK cells treated with 100 pmol c-Myc–specific siRNA-1, c-Myc–specific siRNA-2, or firefly luciferase–specific siRNA (control siRNA) were transfected with a CagA or EGFP expression vector. Cells were stained with an anti-p21 antibody (red, top, confocal x-y view) or an anti–ZO-1 antibody (bottom, confocal x-z view). Bars, 10 µm. (E, right) Anti–c-Myc immunoblotting of polarized MDCK cells treated with 100 pmol c-Myc siRNA or 100 pmol of control siRNA (top). Percentage of p21-positive cells in c-Myc knockdown MDCK cells expressing CagA or EGFP (bottom). Error bars indicate mean ± SD. $n = 3$. *, $P < 0.05$. Representative staining (A and E) and gel (B–E) images from three independent experiments are shown.

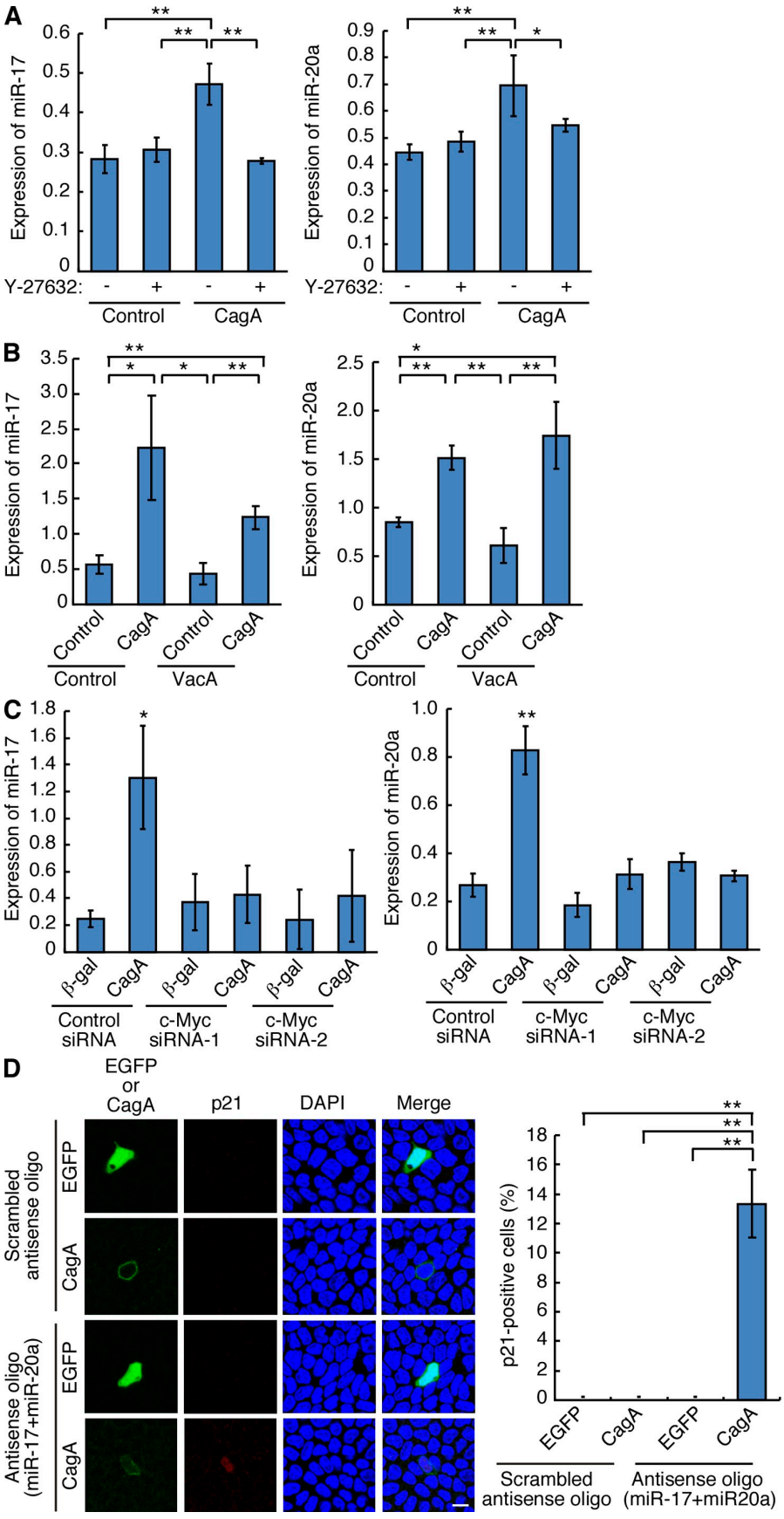

Figure 9. Induction of p21-targeting microRNAs upon expression of CagA in polarized epithelial cells. (A) Polarized MDCK cells were infected with adenovirus transducing CagA or β-galactosidase (control). At 6 h after infection, cells were treated with or without Y-27632 at a final concentration of 50 µM and were cultured for an additional 18 h. Expression of miR-17 (left) or miR-20a (right) was quantified by real-time PCR. Error bars indicate mean ± SD. $n = 3$ for miR-17, $n = 4$ for miR-20a. **, $P < 0.01$; *, $P < 0.05$. (B) Polarized MDCK cells were infected with an adenovirus transducing CagA or β-galactosidase (control). At 6 h after infection, cells were treated with or without 5 µg/ml of acid-activated VacA and cultured for an additional 18 h. Expression of miR-17 (left) or miR-20a (right) was quantified by real-time PCR. Error bars indicate mean ± SD. $n = 3$. **, $P < 0.01$; *, $P < 0.05$. (C) Polarized MDCK cells were treated with c-Myc– or firefly luciferase-specific siRNA (control siRNA) and then infected with an adenovirus transducing CagA or β-galactosidase (β-gal). Expression of miR-17 (left) or miR-20a (right) was quantified by real-time PCR. Error bars indicate mean ± SD. $n = 3$. **, $P < 0.01$; *, $P < 0.05$. (D, left) Polarized MDCK cells were transfected with antisense oligonucleotide for miR-17 and miR-20a or scrambled antisense oligonucleotide together with CagA or EGFP vector. Transfected cells were then stained with anti-p21 antibody (red), anti-HA antibody (green), and DAPI (blue). Bar, 10 µm. (D, right) Percentage of p21-positive cells in MDCK cells expressing EGFP or CagA. Error bars indicate mean ± SD. $n = 3$. **, $P < 0.01$. Representative staining images from three independent experiments are shown in D.

epithelial cells not only elicits Erk activation but also generates a co-lateral signal that overrides the oncogenic stress-induced cell senescence (Fig. S8). Hence, a single bacterial protein creates an integrated biological output that mimics oncogene collaboration (i.e., *ras* and *myc* collaboration) to bypass senescence and yet induce forced mitogenesis in an epithelial-polarity context-dependent manner.

Deregulated Erk activation by gain-of-function mutations in oncogenes, especially those constituting the Ras–Erk pathway, leads to premature senescence in primary cells through induction of CDK inhibitors such as p21 and p16 (Sewing et al., 1997; Woods et al., 1997; Roovers and Assoian, 2000). Oncogene-induced senescence has been considered to act as a cell-autonomous protective response against neoplastic transformation (Ben-Porath and Weinberg, 2005; Zhang, 2007). Accumulation of p21 is primarily a result of Erk-mediated phosphorylation and activation of Sp1 (Kim and Lim, 2009; Tan and Khachigian, 2009), which directs p21 transcription. Like endogenous oncogenes, *H. pylori* CagA aberrantly activates Erk signaling by deregulating cellular proteins, such as SHP-2, and thereby exerts oncogenic stress when expressed in nonpolarized epithelial cells, hampering its potential as a mitogenic oncoprotein (Tsutsumi et al., 2003; Higashi et al., 2004; Murata-Kamiya et al., 2007).

In the *H. pylori*–infected stomach, CagA is delivered into the polarized epithelial monolayer via type IV secretion. Upon delivery, CagA deregulates Erk signaling and, at the same time, inhibits the polarity-regulating kinase PAR1/MARK, resulting in disruption of tight junctions and loss of apical-basal epithelial polarity. As a consequence, CagA-expressing cells extrude from the polarized epithelial monolayer (Amieva et al., 2003; Bagnoli et al., 2005; Saadat et al., 2007). Similar cell extrusion occurs when Ras- or Src-transformed cells are surrounded by polarized normal epithelial cells both in vitro and in vivo (Hogan et al., 2009; Kajita et al., 2010), indicating that CagA-expressing cells have acquired malignant properties shared by Ras- or Src-transformed cells. Intriguingly, CagA-positive cells that have expelled from the polarized monolayer start DNA synthesis and subsequent cell multiplication in response to CagA-activated Erk signaling without causing p21 accumulation, even after they become nonpolarized (Fig. 2). This indicates that, during transition from a polarized state to a nonpolarized state, CagA-expressing epithelial cells acquire the ability to override Erk-dependent p21 accumulation independent of cell polarity status. Once established, this p21-inhibitory mechanism is kept active until the CagA level decreases below a certain threshold. Although the mechanism underlying this phenomenon needs further investigation, the results of the present study suggested that sustained membrane localization of active GEF-H1 plays an important role in this process. In polarized epithelial cells, GEF-H1 is recruited to the membrane, whereas in nonpolarized cells it is distributed to the cytoplasm and its activity is inhibited by binding with microtubules. *H. pylori*–delivered CagA localizes to the inner surface of the plasma membrane by interacting with phosphatidylserine (Murata-Kamiya et al., 2010). In polarized epithelial cells, membrane-localized CagA binds and inhibits PAR1 and thereby provokes junctional and polarity defects, which in turn elicit the activation of GEF-H1 via its dissociation from the inhibitor cingulin. Released GEF-H1 then interacts with the membrane-tethered CagA through PAR1, keeping active GEF-H1 localized to the membrane. Sustained membrane localization of active GEF-H1, which is achieved only when CagA has been delivered into polarized epithelial cells, may enable continued inhibition of p21 accumulation even after cells become nonpolarized.

Activated Erk signaling also plays an essential role in CagA-induced cell elongation, known as the hummingbird phenotype, in nonpolarized gastric epithelial cells such as AGS cells (Higashi et al., 2002, 2004). Notably, *H. pylori* infection can activate Erk signaling independent of CagA, probably via stimulation of growth factor receptors such as EGF-R and HER2/neu (Keates et al., 2001; Wallasch et al., 2002; Du et al., 2007; Tegtmeyer et al., 2009). This *H. pylori* infection–activated Erk signaling acts together with CagA-activated Erk signaling to enhance induction of the hummingbird phenotype by CagA (Tegtmeyer et al., 2009). These observations indicate that infection with *cagA*-positive *H. pylori* causes a higher level of Erk activation than that achieved by CagA alone, resulting in greater accumulation of p21 in nonpolarized cells and stronger mitogenesis in polarized epithelial cells. It has also been reported that CagA and VacA down-regulate each other's effects on epithelial cells. VacA diminishes induction of the hummingbird phenotype upon *cagA*-positive *H. pylori* infection by specific inhibition of EGF-R and neu-dependent Erk activation (Argent et al., 2008; Tegtmeyer et al., 2009). Notably, however, VacA does not directly inhibit the ability of CagA to induce the hummingbird phenotype (Yokoyama et al., 2005). Consistent with these notions, we found in this paper that VacA does not influence the effect of CagA on p21 expression in both polarized and nonpolarized MDCK cells.

CagA-expressing cells expelled from the polarized epithelial monolayer show morphological transformation to an invasive mesenchymal phenotype, a phenomenon known as EMT. Initiation of the EMT program is usually associated with loss of functional E-cadherin, which in many cases is achieved through transrepression by EMT-inducing transcription factors such as Twist, Snail, and Zeb1 (Acloque et al., 2009; Kalluri and Weinberg, 2009). However, recent studies also suggest that disorganization of tight junctions could trigger the EMT program as well (Barrios-Rodiles et al., 2005; Ozdamar et al., 2005). Accordingly, CagA-mediated disruption of tight junctions may trigger the EMT program in polarized epithelial cells. Reported interaction of CagA with E-cadherin, which impairs E-cadherin activity, may also contribute to the progression of EMT (Murata-Kamiya et al., 2007; Kurashima et al., 2008; Oliveira et al., 2009). CagA-activated Erk signaling could further promote EMT through disassembly of adherens junctions as well as elevated cell motility (Zavadil et al., 2001). During EMT, CagA-expressing cells become positive for mesenchymal markers, although they neither down-regulate epithelial markers nor induce

EMT-inducing transcription factors. Hence, CagA-triggered EMT represents an aberrantly dedifferentiated/transdifferentiated cellular status.

Recent studies have indicated a relationship among p21, senescence, and EMT. EMT-inducing transcription factor Twist inhibits p21 (Ansieau et al., 2008). Conversely, p21 reverses Twist-mediated E-cadherin repression (Li et al., 2009). Mice deficient in another EMT-inducing transcription factor Zeb1 exhibit an EMT-like change and *Zeb1*-null mouse embryonic fibroblasts show accumulation of p21 (Liu et al., 2008). In addition, EMT confers resistance to oncogene-induced cell senescence by suppressing accumulation of p21 and/or p16 (Ansieau et al., 2008), whereas elevated p21 attenuates Ras- and c-Myc–dependent induction of EMT (Liu et al., 2009a). These observations strongly suggest that CDK inhibitors, such as p21, act as a molecular switch that determines cell fate, either senescence or EMT, in response to oncogenic insults. A key question is, therefore, how *H. pylori* CagA regulates p21 in an epithelial polarity-dependent manner. We found in this work that RhoA is a key determinant in this process. We also found that the GEF-H1–cingulin complex plays a critical role in the activation of RhoA after expression of CagA in polarized epithelial cells. GEF-H1 is a RhoA-specific GDP/GTP exchanging factor whose activity is inhibited by interaction with cingulin (Aijaz et al., 2005; Birkenfeld et al., 2008). During apical-basal polarization of epithelial cells, the GEF-H1–cingulin complex is formed and concentrated to the tight junctions. Expression of CagA in polarized epithelial cells elicits junctional and polarity defects, which enforce dissociation of cingulin from the GEF-H1–cingulin complex. Being liberated from constraints by cingulin, GEF-H1 stimulates RhoA, which results in the suppression of p21 accumulation (Auer et al., 1998; Olson et al., 1998).

Our findings also provide an insight into the mechanisms underlying suppression of p21 accumulation by activated RhoA. GEF-H1–activated RhoA stimulates the Rho kinase ROCK, which in turn increases the active form of c-Myc. It has been reported that c-Myc inhibits *p21* transcription via multiple distinct mechanisms (Wanzel et al., 2003). Notably, however, inhibition of p21 by RhoA involves posttranscriptional mechanisms (Coleman et al., 2006). In fact, we found that c-Myc induces microRNAs—miR-17 and miR-20a—that target *p21* mRNA and that these microRNAs plays a dominant role in the inhibition of CagA/Erk-dependent p21 accumulation when CagA is expressed in polarized epithelial cells.

A series of studies on *Drosophila melanogaster* tumor suppressor genes demonstrated a role for epithelial polarity in preventing tumor development in flies (Tapon, 2003; Bilder, 2004). Consistently, loss of epithelial polarity is a hallmark of carcinomas in mammals. Nevertheless, the actual contribution of polarity defects in mammalian carcinogenesis has remained uncertain. The present work has demonstrated a causal relationship between epithelial polarity and proliferation control, providing evidence for a tumor-suppressive role of polarized epithelial cells. Disruption of cell–cell junctions and subsequent loss of epithelial polarity liberate cells from growth-inhibitory cues through activation of the GEF-H1–RhoA–ROCK–c-Myc–microRNA–p21 signaling axis, a long-sought signaling pathway which directly links epithelial polarity and the cell cycle. We suspect that deregulation of the identified GEF-H1–RhoA–ROCK–c-Myc–microRNA–p21 axis is broadly and substantially involved in the neoplastic transformation of epithelial cells, other than gastric epithelial cells.

CagA-mediated increase in the number of abnormal epithelial cells that have undergone EMT would have a significant impact on the physiological functions of the stomach mucosa such as gastric acid secretion. For *H. pylori*, reduced acidity should be of great advantage for long-term colonization in the stomach. Meanwhile, Mani et al. (2008) recently reported that EMT allocates epithelial cells with malignant characteristics, indicating that CagA-expressing epithelial cells that have undergone EMT acquire malignant traits. Accordingly, an unexpected adverse effect of CagA, which primarily acts for the better life of *H. pylori*, is that it allows continuous generation and expansion of a cancer-predisposed cell population in the *H. pylori*–infected stomach.

MATERIALS AND METHODS

Cell lines. MKN28, AGS, COS-7, and MDCK (MDCK II) cells were cultured as previously described (Higashi et al., 2002; Murata-Kamiya et al., 2007; Saadat et al., 2007). WT-A10 cell is an MKN28-derived stable transfectant clone that inducibly expresses CagA using a tet-off system (Murata-Kamiya et al., 2007). The p21sh-6-12 cell is a WT-A10–derived clone made by stable transfection of pSUPER-p21, an expression vector for p21-specific shRNA. MDCK cells were grown on Transwell filters (Corning) to make polarized epithelial monolayer. MDCK cells that inducibly express CagA were established using Tet-on Advanced Inducible Gene Expression System (Takara Bio Inc.). In brief, MDCK cells were transfected with pTet-On-Advanced Vector and were selected in the presence of 800 μg/ml G418. Transfectants carrying pTet-On-Advanced were then transfected with pTRE-tight-CagA and a drug-resistant gene (pBabe-puro) and were selected in the presence of 1 μg/ml puromycin. MDCK transfectants that inducibly express in the presence of 0.2 μg/ml of a tetracycline analogue, Dox, were single cell cloned by limiting dilution method.

Expression vectors. Mammalian expression vectors for WT CagA, PR-CagA, and a CagA mutant that lacks the PAR1/MARK-interacting sequence (CagA-ΔCM/MKI) were described previously (Higashi et al., 2002; Saadat et al., 2007). Human cDNA for GEF-H1 (Fujishiro et al., 2008) was provided by M. Kohno (Nagasaki University, Nagasaki, Japan). An expression vector for a RhoA-specific FRET probe, pRaichu-RhoA (1298x; Yoshizaki et al., 2003), was provided by M. Matsuda (Kyoto University, Kyoto, Japan). Plasmids were transfected into cells as previously described (Higashi et al., 2002). Recombinant adenoviruses that express a RhoA FRET probe, WT CagA, and β-galactosidase were generated using ViraPower Adenoviral Expression System (Invitrogen).

Antibodies, inhibitors, immunoprecipitation, and immunoblotting. Anti-HA (3F10; Roche), anti-Flag (Sigma-Aldrich), anti-c-Myc (9E10; Santa Cruz Biotechnology, Inc.), anti-T7 (sc-7270; Santa Cruz Biotechnology, Inc.), anti-RhoA (sc-179; Santa Cruz Biotechnology, Inc.), anti-RhoA (Millipore), anti-actin (sc-1615; Santa Cruz Biotechnology, Inc.), anti-ERK1 (sc-93; Santa Cruz Biotechnology, Inc.), anti–p-ERK (sc-7383; Santa Cruz Biotechnology, Inc.), anti-p21 (sc-397; Santa Cruz Biotechnology, Inc.), anti-bromodeoxyuridine (Roche), anti-CagA (AUSTRAL Biologicals), anti-HA (6E2; Cell Signaling Technology), anti–phospho-c-Myc (Cell Signaling Technology), anti–c-Myc (Cell Signaling Technology), anti–GEF-H1 (B4/7; Hycult Biotech), anti–α-tubulin (sc-53029; Santa Cruz Biotechnology, Inc.), anti–Snail 1 (sc-28199; Santa Cruz Biotechnology, Inc.), anti-Twist

(3E11; Abnova), anti–ZO-1 (Invitrogen), anti–α-catenin (BD), anti–β-catenin (BD), anti–γ-catenin (BD), anti-vimentin (V9; Thermo Fisher Scientific), anti-fibronectin (BD), anti–E-cadherin (BD), anti–N-cadherin (BD), and anti-cingulin (Invitrogen) antibodies were used in this study. A rabbit anti-PAR1b antibody was provided by S. Ohno (Yokohama City University, Yokohama City, Japan). MEK inhibitor U0126 and its control U0124 (EMD) were used at the final concentration of 25 μM. Cell permeable C3 transferase from *Clostridium botulinum* (Cytoskeleton, Inc.) was used at the final concentration of 5 μg/ml. ROCK inhibitor Y-27632 was purchased from EMD and was used at the final concentration of 50 μM. Immunoprecipitation and immunoblotting were performed as previously described (Higashi et al., 2002).

Flow cytometric analysis. Cells were collected by trypsinization, washed with PBS, and fixed in 70% cold ethanol at −20°C overnight. After centrifugation, cells were washed with PBS and treated for 20 min at 37°C with 0.5 mg/ml RNase A. Cells were stained at room temperature with 50 μg/ml propidium iodide and subjected to flow cytometric analysis using FACScan and Cell Quest software (BD).

Confocal microscopy. Cells were fixed and permeabilized as previously described (Higashi et al., 2002). The cells were then treated with primary antibodies and visualized with Alexa Fluor conjugate secondary antibodies (Invitrogen). Images were captured with a confocal microscope system (Olympus).

BrdU incorporation assay. Nonpolarized or polarized MDCK cells were transfected with expression vectors. At 12 h after transfection, 10 μM BrdU was added to the culture and cells were labeled with BrdU for an additional 15 h. After fixation and permeabilization, cells were treated with 5 U/μl DNase for 1 h at 37°C and were stained with an anti-BrdU antibody.

FRET assay. MDCK II cells were transfected with pRaichu-RhoA together with expression vector. At 24 h after transfection, cells were washed and lysed as previously described (Yoshizaki et al., 2003). Cell lysates were centrifuged and transferred into 96-well plates. Fluorescence was measured with a fluorescence spectrophotometer (LS 50; PerkinElmer) using an excitation wavelength of 430 nm. The ratios of emission at 530/475 nm were calculated. In several experiments, polarized MDCK II cells were cultured in calcium-free medium for 24 h and then coinfected with recombinant adenoviruses that transduce a FRET probe for RhoA and CagA-WT or β-galactosidase. At 24 h after infection, cells were lysed and fluorescence was measured with a fluorescence spectrophotometer.

RhoA pulldown assay. RhoA activity was determined using Rho Assay Reagent kit according to the manufacturer's instruction (Millipore). Quantitation of RhoA bands obtained by anti-RhoA immunoblotting was performed using a luminescence image analyzer (LAS-4000 IR multi color; Fujifilm).

siRNA experiment. GEF-H1–specific siRNA-1 (5′-GCUUUACAAGGAGCUGUAUTT-3′) and GEF-H1–specific siRNA-2 (5′-CCAGGAGAAAGGGAUGUTT-3′) or c-Myc–specific siRNA-1 (5′-GAGGCGAACACACAACGUCTT-3′) and c-Myc–specific siRNA-2 (5′-GCGGCGAGAACAGUUGAAATT-3′) were synthesized. p21-specific siRNA (Hs-CDKN1A-5 FlexiTube siRNA) was purchased from QIAGEN. Each 100-pmol siRNA was transfected into cells. At 12 h after transfection, cells were reseeded on Transwell. After 3 d of culture, cells were transfected with plasmid vectors. At 27 h after transfection, cells were fixed and stained with anti-p21 antibody.

Senescence-associated (SA) β-galactosidase assay. CagA-inducible MKN28 or CagA-inducible MDCK cells were cultured for 5 d in the presence or absence of Dox. Cells were then washed with PBS, fixed with 3% formaldehyde, and incubated overnight with staining buffer (1 mg/ml X-Gal, 40 mM citric acid/sodium phosphate, pH 6.0, 150 mM NaCl, 2 mM $MgCl_2$, 5 mM $K_3Fe(CN)_6$, and 5 mM $K_4Fe(CN)_6$) for detecting SA-β-galactosidase activity.

Real-time RT-PCR. Expression of mature microRNAs was measured using TaqMan MicroRNA Assays (Applied Biosystems). In brief, total RNA was extracted with the use of TRIzol reagent (Invitrogen) according to the manufacturer's protocol. Reverse transcription was conducted with TaqMan MicroRNA Reverse Transcription kit (Applied Biosystems) using specific stem-loop primer for miR-17, miR-20a, and RNU6B (control). Real-time PCR was performed with LightCycler 480 (Roche) using LightCycler Taqman master (Roche) and TaqMan MicroRNA assay system (Applied Biosystems). Expression of microRNAs was normalized using U6 snRNA (*RNU6B*) as a control.

Antisense oligonucleotides. Antisense oligonucleotide against miR-17 (5′-CTACAAGTGCCTTCACTGCAGT-3′), antisense oligonucleotide against miR-20a (5′-CTACCTGCACTATAAGCACTTTA-3′), and control oligonucleotide (5′-TAACGTCACTTCGACTGAAGTGCT-3′) were synthesized with modification of LNA (locked nucleic acid; 2′-O and 4′-C methylene bridge modification) at G and C residues (GeneDesign Inc.). Polarized MDCK cells were cotransfected with an antisense oligonucleotide and an expression vector. 27 h after transfection, cells were fixed and stained with anti-p21 and anti-HA antibodies.

Statistics. Statistical analyses were performed by the Student's *t* test.

Online supplemental material. Fig. S1 shows inhibition of cell proliferation by CagA in nonpolarized AGS gastric epithelial cells. Fig. S2 shows representative staining images of nonpolarized or polarized MDCK cells. Fig. S3 shows inhibition of proliferation by CagA in nonpolarized MDCK cells. Fig. S4 shows inhibition of proliferation by CagA in MKN28 cells cultured on Transwell filters. Fig. S5 shows induction of proliferation by CagA in polarized MDCK cells. Fig. S6 shows requirement of GEF-H1 for the inhibition of CagA-mediated p21 accumulation in polarized epithelial cells. Fig. S7 shows induction of p21-targeting microRNAs upon calcium depletion by activation of the ROCK–c-Myc pathway. Fig. S8 summarizes a model for epithelial polarity-dependent cellular response to CagA. Online supplemental material is available at http://www.jem.org/cgi/content/full/jem.20100602/DC1.

We thank Drs. Michiyuki Matsuda, Jun-ichi Miyazaki, Michiaki Kohno, and Shigeo Ohno for plasmids and antibodies. We also thank Dr. Tadatsugu Taniguchi for experimental help.

This work was supported by Grants-in-Aid for Scientific Research from the Ministry of Education, Culture, Sports, Science and Technology (MEXT) of Japan and by the Mitsubishi Foundation Research Grant.

The authors declare that they have no conflicting financial interests.

Submitted: 25 March 2010
Accepted: 26 August 2010

REFERENCES

Acloque, H., M.S. Adams, K. Fishwick, M. Bronner-Fraser, and M.A. Nieto. 2009. Epithelial-mesenchymal transitions: the importance of changing cell state in development and disease. *J. Clin. Invest.* 119:1438–1449. doi:10.1172/JCI38019

Adnane, J., F.A. Bizouarn, Y. Qian, A.D. Hamilton, and S.M. Sebti. 1998. p21($^{WAF1/CIP1}$) is upregulated by the geranylgeranyltransferase I inhibitor GGTI-298 through a transforming growth factor β- and Sp1-responsive element: involvement of the small GTPase rhoA. *Mol. Cell. Biol.* 18:6962–6970.

Aijaz, S., F. D'Atri, S. Citi, M.S. Balda, and K. Matter. 2005. Binding of GEF-H1 to the tight junction-associated adaptor cingulin results in inhibition of Rho signaling and G1/S phase transition. *Dev. Cell.* 8:777–786. doi:10.1016/j.devcel.2005.03.003

Amieva, M.R., R. Vogelmann, A. Covacci, L.S. Tompkins, W.J. Nelson, and S. Falkow. 2003. Disruption of the epithelial apical-junctional

complex by *Helicobacter pylori* CagA. *Science*. 300:1430–1434. doi:10.1126/science.1081919

Ansieau, S., J. Bastid, A. Doreau, A.P. Morel, B.P. Bouchet, C. Thomas, F. Fauvet, I. Puisieux, C. Doglioni, S. Piccinin, et al. 2008. Induction of EMT by twist proteins as a collateral effect of tumor-promoting inactivation of premature senescence. *Cancer Cell*. 14:79–89. doi:10.1016/j.ccr.2008.06.005

Argent, R.H., R.J. Thomas, D.P. Letley, M.G. Rittig, K.R. Hardie, and J.C. Atherton. 2008. Functional association between the *Helicobacter pylori* virulence factors VacA and CagA. *J. Med. Microbiol.* 57:145–150. doi:10.1099/jmm.0.47465-0

Asahi, M., T. Azuma, S. Ito, Y. Ito, H. Suto, Y. Nagai, M. Tsubokawa, Y. Tohyama, S. Maeda, M. Omata, et al. 2000. *Helicobacter pylori* CagA protein can be tyrosine phosphorylated in gastric epithelial cells. *J. Exp. Med.* 191:593–602. doi:10.1084/jem.191.4.593

Auer, K.L., J.S. Park, P. Seth, R.J. Coffey, G. Darlington, A. Abo, M. McMahon, R.A. Depinho, P.B. Fisher, and P. Dent. 1998. Prolonged activation of the mitogen-activated protein kinase pathway promotes DNA synthesis in primary hepatocytes from $p21^{Cip-1/WAF1}$-null mice, but not in hepatocytes from $p16^{INK4a}$-null mice. *Biochem. J.* 336:551–560.

Backert, S., and M. Selbach. 2005. Tyrosine-phosphorylated bacterial effector proteins: the enemies within. *Trends Microbiol.* 13:476–484. doi:10.1016/j.tim.2005.08.002

Backert, S., E. Ziska, V. Brinkmann, U. Zimny-Arndt, A. Fauconnier, P.R. Jungblut, M. Naumann, and T.F. Meyer. 2000. Translocation of the *Helicobacter pylori* CagA protein in gastric epithelial cells by a type IV secretion apparatus. *Cell. Microbiol.* 2:155–164. doi:10.1046/j.1462-5822.2000.00043.x

Bagnoli, F., L. Buti, L. Tompkins, A. Covacci, and M.R. Amieva. 2005. *Helicobacter pylori* CagA induces a transition from polarized to invasive phenotypes in MDCK cells. *Proc. Natl. Acad. Sci. USA*. 102:16339–16344. doi:10.1073/pnas.0502598102

Barrios-Rodiles, M., K.R. Brown, B. Ozdamar, R. Bose, Z. Liu, R.S. Donovan, F. Shinjo, Y. Liu, J. Dembowy, I.W. Taylor, et al. 2005. High-throughput mapping of a dynamic signaling network in mammalian cells. *Science*. 307:1621–1625. doi:10.1126/science.1105776

Bartel, D.P. 2004. MicroRNAs: genomics, biogenesis, mechanism, and function. *Cell*. 116:281–297. doi:10.1016/S0092-8674(04)00045-5

Ben-Porath, I., and R.A. Weinberg. 2005. The signals and pathways activating cellular senescence. *Int. J. Biochem. Cell Biol.* 37:961–976. doi:10.1016/j.biocel.2004.10.013

Bilder, D. 2004. Epithelial polarity and proliferation control: links from the *Drosophila* neoplastic tumor suppressors. *Genes Dev.* 18:1909–1925. doi:10.1101/gad.1211604

Birkenfeld, J., P. Nalbant, S.H. Yoon, and G.M. Bokoch. 2008. Cellular functions of GEF-H1, a microtubule-regulated Rho-GEF: is altered GEF-H1 activity a crucial determinant of disease pathogenesis? *Trends Cell Biol.* 18:210–219. doi:10.1016/j.tcb.2008.02.006

Brajenovic, M., G. Joberty, B. Küster, T. Bouwmeester, and G. Drewes. 2004. Comprehensive proteomic analysis of human Par protein complexes reveals an interconnected protein network. *J. Biol. Chem.* 279:12804–12811. doi:10.1074/jbc.M312171200

Cabral, M.M., C.A. Oliveira, C.M. Mendes, J. Guerra, D.M. Queiroz, G.A. Rocha, A.M. Rocha, and A.M. Nogueira. 2007. Gastric epithelial cell proliferation and *cagA* status in *Helicobacter pylori* gastritis at different gastric sites. *Scand. J. Gastroenterol.* 42:545–554. doi:10.1080/00365520601014034

Chang, Y.C., P. Nalbant, J. Birkenfeld, Z.F. Chang, and G.M. Bokoch. 2008. GEF-H1 couples nocodazole-induced microtubule disassembly to cell contractility via RhoA. *Mol. Biol. Cell*. 19:2147–2153. doi:10.1091/mbc.E07-12-1269

Churin, Y., L. Al-Ghoul, O. Kepp, T.F. Meyer, W. Birchmeier, and M. Naumann. 2003. *Helicobacter pylori* CagA protein targets the c-Met receptor and enhances the motogenic response. *J. Cell Biol.* 161:249–255. doi:10.1083/jcb.200208039

Coleman, M.L., R.M. Densham, D.R. Croft, and M.F. Olson. 2006. Stability of $p21^{Waf1/Cip1}$ CDK inhibitor protein is responsive to RhoA-mediated regulation of the actin cytoskeleton. *Oncogene*. 25:2708–2716. doi:10.1038/sj.onc.1209322

Du, Y., K. Danjo, P.A. Robinson, and J.E. Crabtree. 2007. In-Cell Western analysis of *Helicobacter pylori*-induced phosphorylation of extracellular-signal related kinase via the transactivation of the epidermal growth factor receptor. *Microbes Infect.* 9:838–846. doi:10.1016/j.micinf.2007.03.004

Fujishiro, S.H., S. Tanimura, S. Mure, Y. Kashimoto, K. Watanabe, and M. Kohno. 2008. ERK1/2 phosphorylate GEF-H1 to enhance its guanine nucleotide exchange activity toward RhoA. *Biochem. Biophys. Res. Commun.* 368:162–167. doi:10.1016/j.bbrc.2008.01.066

García-Mata, R., K. Wennerberg, W.T. Arthur, N.K. Noren, S.M. Ellerbroek, and K. Burridge. 2006. Analysis of activated GAPs and GEFs in cell lysates. *Methods Enzymol.* 406:425–437. doi:10.1016/S0076-6879(06)06031-9

Hatakeyama, M. 2008. SagA of CagA in *Helicobacter pylori* pathogenesis. *Curr. Opin. Microbiol.* 11:30–37. doi:10.1016/j.mib.2007.12.003

Higashi, H., R. Tsutsumi, S. Muto, T. Sugiyama, T. Azuma, M. Asaka, and M. Hatakeyama. 2002. SHP-2 tyrosine phosphatase as an intracellular target of *Helicobacter pylori* CagA protein. *Science*. 295:683–686. doi:10.1126/science.1067147

Higashi, H., A. Nakaya, R. Tsutsumi, K. Yokoyama, Y. Fujii, S. Ishikawa, M. Higuchi, A. Takahashi, Y. Kurashima, Y. Teishikata, et al. 2004. *Helicobacter pylori* CagA induces Ras-independent morphogenetic response through SHP-2 recruitment and activation. *J. Biol. Chem.* 279:17205–17216. doi:10.1074/jbc.M309964200

Hogan, C., S. Dupré-Crochet, M. Norman, M. Kajita, C. Zimmermann, A.E. Pelling, E. Piddini, L.A. Baena-López, J.P. Vincent, Y. Itoh, et al. 2009. Characterization of the interface between normal and transformed epithelial cells. *Nat. Cell Biol.* 11:460–467. doi:10.1038/ncb1853

Inomata, M., H. Tagawa, Y.M. Guo, Y. Kameoka, N. Takahashi, and K. Sawada. 2009. MicroRNA-17-92 down-regulates expression of distinct targets in different B-cell lymphoma subtypes. *Blood*. 113:396–402. doi:10.1182/blood-2008-07-163907

Kajita, M., C. Hogan, A.R. Harris, S. Dupré-Crochet, N. Itasaki, K. Kawakami, G. Charras, M. Tada, and Y. Fujita. 2010. Interaction with surrounding normal epithelial cells influences signalling pathways and behaviour of Src-transformed cells. *J. Cell Sci.* 123:171–180. doi:10.1242/jcs.057976

Kalluri, R., and R.A. Weinberg. 2009. The basics of epithelial-mesenchymal transition. *J. Clin. Invest.* 119:1420–1428. doi:10.1172/JCI39104

Keates, S., S. Sougioultzis, A.C. Keates, D. Zhao, R.M. Peek Jr., L.M. Shaw, and C.P. Kelly. 2001. *cag+ Helicobacter pylori* induce transactivation of the epidermal growth factor receptor in AGS gastric epithelial cells. *J. Biol. Chem.* 276:48127–48134.

Kim, H.S., and I.K. Lim. 2009. Phosphorylated extracellular signal-regulated protein kinases 1 and 2 phosphorylate Sp1 on serine 59 and regulate cellular senescence via transcription of $p21^{Sdi1/Cip1/Waf1}$. *J. Biol. Chem.* 284:15475–15486. doi:10.1074/jbc.M808734200

Krendel, M., F.T. Zenke, and G.M. Bokoch. 2002. Nucleotide exchange factor GEF-H1 mediates cross-talk between microtubules and the actin cytoskeleton. *Nat. Cell Biol.* 4:294–301. doi:10.1038/ncb773

Kurashima, Y., N. Murata-Kamiya, K. Kikuchi, H. Higashi, T. Azuma, S. Kondo, and M. Hatakeyama. 2008. Deregulation of β-catenin signal by *Helicobacter pylori* CagA requires the CagA-multimerization sequence. *Int. J. Cancer*. 122:823–831. doi:10.1002/ijc.23190

Li, Q.Q., J.D. Xu, W.J. Wang, X.X. Cao, Q. Chen, F. Tang, Z.Q. Chen, X.P. Liu, and Z.D. Xu. 2009. Twist1-mediated adriamycin-induced epithelial-mesenchymal transition relates to multidrug resistance and invasive potential in breast cancer cells. *Clin. Cancer Res.* 15:2657–2665. doi:10.1158/1078-0432.CCR-08-2372

Liberto, M., D. Cobrinik, and A. Minden. 2002. Rho regulates $p21^{(CIP1)}$, cyclin D1, and checkpoint control in mammary epithelial cells. *Oncogene*. 21:1590–1599. doi:10.1038/sj.onc.1205242

Liu, Y., S. El-Naggar, D.S. Darling, Y. Higashi, and D.C. Dean. 2008. Zeb1 links epithelial-mesenchymal transition and cellular senescence. *Development*. 135:579–588. doi:10.1242/dev.007047

Liu, M., M.C. Casimiro, C. Wang, L.A. Shirley, X. Jiao, S. Katiyar, X. Ju, Z. Li, Z. Yu, J. Zhou, et al. 2009a. $p21^{CIP1}$ attenuates Ras- and c-Myc-dependent breast tumor epithelial mesenchymal transition and cancer stem cell-like gene expression in vivo. *Proc. Natl. Acad. Sci. USA*. 106:19035–19039. doi:10.1073/pnas.0910009106

Liu, S., R.H. Goldstein, E.M. Scepansky, and M. Rosenblatt. 2009b. Inhibition of rho-associated kinase signaling prevents breast cancer metastasis to human bone. *Cancer Res*. 69:8742–8751. doi:10.1158/0008-5472.CAN-09-1541

Lu, H.S., Y. Saito, M. Umeda, N. Murata-Kamiya, H.M. Zhang, H. Higashi, and M. Hatakeyama. 2008. Structural and functional diversity in the PAR1b/MARK2-binding region of *Helicobacter pylori* CagA. *Cancer Sci*. 99:2004–2011. doi:10.1111/j.1349-7006.2008.00950.x

Lu, H., N. Murata-Kamiya, Y. Saito, and M. Hatakeyama. 2009. Role of partitioning-defective 1/microtubule affinity-regulating kinases in the morphogenetic activity of *Helicobacter pylori* CagA. *J. Biol. Chem*. 284:23024–23036. doi:10.1074/jbc.M109.001008

Mani, S.A., W. Guo, M.J. Liao, E.N. Eaton, A. Ayyanan, A.Y. Zhou, M. Brooks, F. Reinhard, C.C. Zhang, M. Shipitsin, et al. 2008. The epithelial-mesenchymal transition generates cells with properties of stem cells. *Cell*. 133:704–715. doi:10.1016/j.cell.2008.03.027

Mimuro, H., T. Suzuki, J. Tanaka, M. Asahi, R. Haas, and C. Sasakawa. 2002. Grb2 is a key mediator of *helicobacter pylori* CagA protein activities. *Mol. Cell*. 10:745–755. doi:10.1016/S1097-2765(02)00681-0

Miura, M., N. Ohnishi, S. Tanaka, K. Yanagiya, and M. Hatakeyama. 2009. Differential oncogenic potential of geographically distinct *Helicobacter pylori* CagA isoforms in mice. *Int. J. Cancer*. 125:2497–2504. doi:10.1002/ijc.24740

Murata-Kamiya, N., Y. Kurashima, Y. Teishikata, Y. Yamahashi, Y. Saito, H. Higashi, H. Aburatani, T. Akiyama, R.M. Peek Jr., T. Azuma, and M. Hatakeyama. 2007. *Helicobacter pylori* CagA interacts with E-cadherin and deregulates the β-catenin signal that promotes intestinal transdifferentiation in gastric epithelial cells. *Oncogene*. 26:4617–4626. doi:10.1038/sj.onc.1210251

Murata-Kamiya, N., K. Kikuchi, T. Hayashi, H. Higashi, and M. Hatakeyama. 2010. *Helicobacter pylori* exploits host membrane phosphatidylserine for delivery, localization, and pathophysiological action of the CagA oncoprotein. *Cell Host Microbe*. 7:399–411. doi:10.1016/j.chom.2010.04.005

Nesić, D., M.C. Miller, Z.T. Quinkert, M. Stein, B.T. Chait, and C.E. Stebbins. 2010. *Helicobacter pylori* CagA inhibits PAR1-MARK family kinases by mimicking host substrates. *Nat. Struct. Mol. Biol*. 17:130–132. doi:10.1038/nsmb.1705

Odenbreit, S., J. Püls, B. Sedlmaier, E. Gerland, W. Fischer, and R. Haas. 2000. Translocation of *Helicobacter pylori* CagA into gastric epithelial cells by type IV secretion. *Science*. 287:1497–1500. doi:10.1126/science.287.5457.1497

Ohnishi, N., H. Yuasa, S. Tanaka, H. Sawa, M. Miura, A. Matsui, H. Higashi, M. Musashi, K. Iwabuchi, M. Suzuki, et al. 2008. Transgenic expression of *Helicobacter pylori* CagA induces gastrointestinal and hematopoietic neoplasms in mouse. *Proc. Natl. Acad. Sci. USA*. 105:1003–1008. doi:10.1073/pnas.0711183105

Oliveira, M.J., A.M. Costa, A.C. Costa, R.M. Ferreira, P. Sampaio, J.C. Machado, R. Seruca, M. Mareel, and C. Figueiredo. 2009. CagA associates with c-Met, E-cadherin, and p120-catenin in a multiproteic complex that suppresses *Helicobacter pylori*-induced cell-invasive phenotype. *J. Infect. Dis*. 200:745–755. doi:10.1086/604727

Olson, M.F., H.F. Paterson, and C.J. Marshall. 1998. Signals from Ras and Rho GTPases interact to regulate expression of $p21^{Waf1/Cip1}$. *Nature*. 394:295–299. doi:10.1038/28425

Ozdamar, B., R. Bose, M. Barrios-Rodiles, H.R. Wang, Y. Zhang, and J.L. Wrana. 2005. Regulation of the polarity protein Par6 by TGFbeta receptors controls epithelial cell plasticity. *Science*. 307:1603–1609. doi:10.1126/science.1105718

Parkin, D.M. 2004. International variation. *Oncogene*. 23:6329–6340. doi:10.1038/sj.onc.1207726

Peek, R.M. Jr., and M.J. Blaser. 2002. *Helicobacter pylori* and gastrointestinal tract adenocarcinomas. *Nat. Rev. Cancer*. 2:28–37. doi:10.1038/nrc703

Peek, R.M. Jr., S.F. Moss, K.T. Tham, G.I. Pérez-Pérez, S. Wang, G.G. Miller, J.C. Atherton, P.R. Holt, and M.J. Blaser. 1997. *Helicobacter pylori* $cagA^+$ strains and dissociation of gastric epithelial cell proliferation from apoptosis. *J. Natl. Cancer Inst*. 89:863–868. doi:10.1093/jnci/89.12.863

Petrocca, F., A. Vecchione, and C.M. Croce. 2008. Emerging role of *miR-106b-25/miR-17-92* clusters in the control of transforming growth factor β signaling. *Cancer Res*. 68:8191–8194. doi:10.1158/0008-5472.CAN-08-1768

Ren, S., H. Higashi, H. Lu, T. Azuma, and M. Hatakeyama. 2006. Structural basis and functional consequence of *Helicobacter pylori* CagA multimerization in cells. *J. Biol. Chem*. 281:32344–32352. doi:10.1074/jbc.M606172200

Roovers, K., and R.K. Assoian. 2000. Integrating the MAP kinase signal into the G1 phase cell cycle machinery. *Bioessays*. 22:818–826. doi:10.1002/1521-1878(200009)22:9<818::AID-BIES7>3.0.CO;2-6

Saadat, I., H. Higashi, C. Obuse, M. Umeda, N. Murata-Kamiya, Y. Saito, H. Lu, N. Ohnishi, T. Azuma, A. Suzuki, et al. 2007. *Helicobacter pylori* CagA targets PAR1/MARK kinase to disrupt epithelial cell polarity. *Nature*. 447:330–333. doi:10.1038/nature05765

Sahai, E., M.F. Olson, and C.J. Marshall. 2001. Cross-talk between Ras and Rho signalling pathways in transformation favours proliferation and increased motility. *EMBO J*. 20:755–766. doi:10.1093/emboj/20.4.755

Segal, E.D., J. Cha, J. Lo, S. Falkow, and L.S. Tompkins. 1999. Altered states: involvement of phosphorylated CagA in the induction of host cellular growth changes by *Helicobacter pylori*. *Proc. Natl. Acad. Sci. USA*. 96:14559–14564. doi:10.1073/pnas.96.25.14559

Sewing, A., B. Wiseman, A.C. Lloyd, and H. Land. 1997. High-intensity Raf signal causes cell cycle arrest mediated by $p21^{Cip1}$. *Mol. Cell. Biol*. 17:5588–5597.

Stein, M., R. Rappuoli, and A. Covacci. 2000. Tyrosine phosphorylation of the *Helicobacter pylori* CagA antigen after cag-driven host cell translocation. *Proc. Natl. Acad. Sci. USA*. 97:1263–1268. doi:10.1073/pnas.97.3.1263

Suzuki, A., and S. Ohno. 2006. The PAR-aPKC system: lessons in polarity. *J. Cell Sci*. 119:979–987. doi:10.1242/jcs.02898

Suzuki, M., H. Mimuro, T. Suzuki, M. Park, T. Yamamoto, and C. Sasakawa. 2005. Interaction of CagA with Crk plays an important role in *Helicobacter pylori*–induced loss of gastric epithelial cell adhesion. *J. Exp. Med*. 202:1235–1247. doi:10.1084/jem.20051027

Tan, N.Y., and L.M. Khachigian. 2009. Sp1 phosphorylation and its regulation of gene transcription. *Mol. Cell. Biol*. 29:2483–2488. doi:10.1128/MCB.01828-08

Tapon, N. 2003. Modeling transformation and metastasis in *Drosophila*. *Cancer Cell*. 4:333–335. doi:10.1016/S1535-6108(03)00279-4

Tegtmeyer, N., D. Zabler, D. Schmidt, R. Hartig, S. Brandt, and S. Backert. 2009. Importance of EGF receptor, HER2/Neu and Erk1/2 kinase signalling for host cell elongation and scattering induced by the *Helicobacter pylori* CagA protein: antagonistic effects of the vacuolating cytotoxin VacA. *Cell. Microbiol*. 11:488–505. doi:10.1111/j.1462-5822.2008.01269.x

Tsutsumi, R., H. Higashi, M. Higuchi, M. Okada, and M. Hatakeyama. 2003. Attenuation of *Helicobacter pylori* CagA x SHP-2 signaling by interaction between CagA and C-terminal Src kinase. *J. Biol. Chem*. 278:3664–3670. doi:10.1074/jbc.M208155200

Wallasch, C., J.E. Crabtree, D. Bevec, P.A. Robinson, H. Wagner, and A. Ullrich. 2002. *Helicobacter pylori*-stimulated EGF receptor transactivation requires metalloprotease cleavage of HB-EGF. *Biochem. Biophys. Res. Commun*. 295:695–701. doi:10.1016/S0006-291X(02)00740-4

Wanzel, M., S. Herold, and M. Eilers. 2003. Transcriptional repression by Myc. *Trends Cell Biol*. 13:146–150. doi:10.1016/S0962-8924(03)00003-5

Watnick, R.S., Y.N. Cheng, A. Rangarajan, T.A. Ince, and R.A. Weinberg. 2003. Ras modulates Myc activity to repress thrombospondin-1 expression and increase tumor angiogenesis. *Cancer Cell*. 3:219–231. doi:10.1016/S1535-6108(03)00030-8

Woods, D., D. Parry, H. Cherwinski, E. Bosch, E. Lees, and M. McMahon. 1997. Raf-induced proliferation or cell cycle arrest is determined by

the level of Raf activity with arrest mediated by $p21^{Cip1}$. *Mol. Cell. Biol.* 17:5598–5611.

Yokoyama, K., H. Higashi, S. Ishikawa, Y. Fujii, S. Kondo, H. Kato, T. Azuma, A. Wada, T. Hirayama, H. Aburatani, and M. Hatakeyama. 2005. Functional antagonism between *Helicobacter pylori* CagA and vacuolating toxin VacA in control of the NFAT signaling pathway in gastric epithelial cells. *Proc. Natl. Acad. Sci. USA.* 102:9661–9666. doi:10.1073/pnas.0502529102

Yoshizaki, H., Y. Ohba, K. Kurokawa, R.E. Itoh, T. Nakamura, N. Mochizuki, K. Nagashima, and M. Matsuda. 2003. Activity of Rho-family GTPases during cell division as visualized with FRET-based probes. *J. Cell Biol.* 162:223–232. doi:10.1083/jcb.200212049

Zavadil, J., M. Bitzer, D. Liang, Y.C. Yang, A. Massimi, S. Kneitz, E. Piek, and E.P. Bottinger. 2001. Genetic programs of epithelial cell plasticity directed by transforming growth factor-beta. *Proc. Natl. Acad. Sci. USA.* 98:6686–6691. doi:10.1073/pnas.111614398

Zeaiter, Z., D. Cohen, A. Müsch, F. Bagnoli, A. Covacci, and M. Stein. 2008. Analysis of detergent-resistant membranes of *Helicobacter pylori* infected gastric adenocarcinoma cells reveals a role for MARK2/Par1b in CagA-mediated disruption of cellular polarity. *Cell. Microbiol.* 10:781–794. doi:10.1111/j.1462-5822.2007.01084.x

Zhang, H. 2007. Molecular signaling and genetic pathways of senescence: Its role in tumorigenesis and aging. *J. Cell. Physiol.* 210:567–574. doi:10.1002/jcp.20919

JEM

SUPPLEMENTAL MATERIAL

Saito et al., http://www.jem.org/cgi/content/full/jem.20100602/DC1

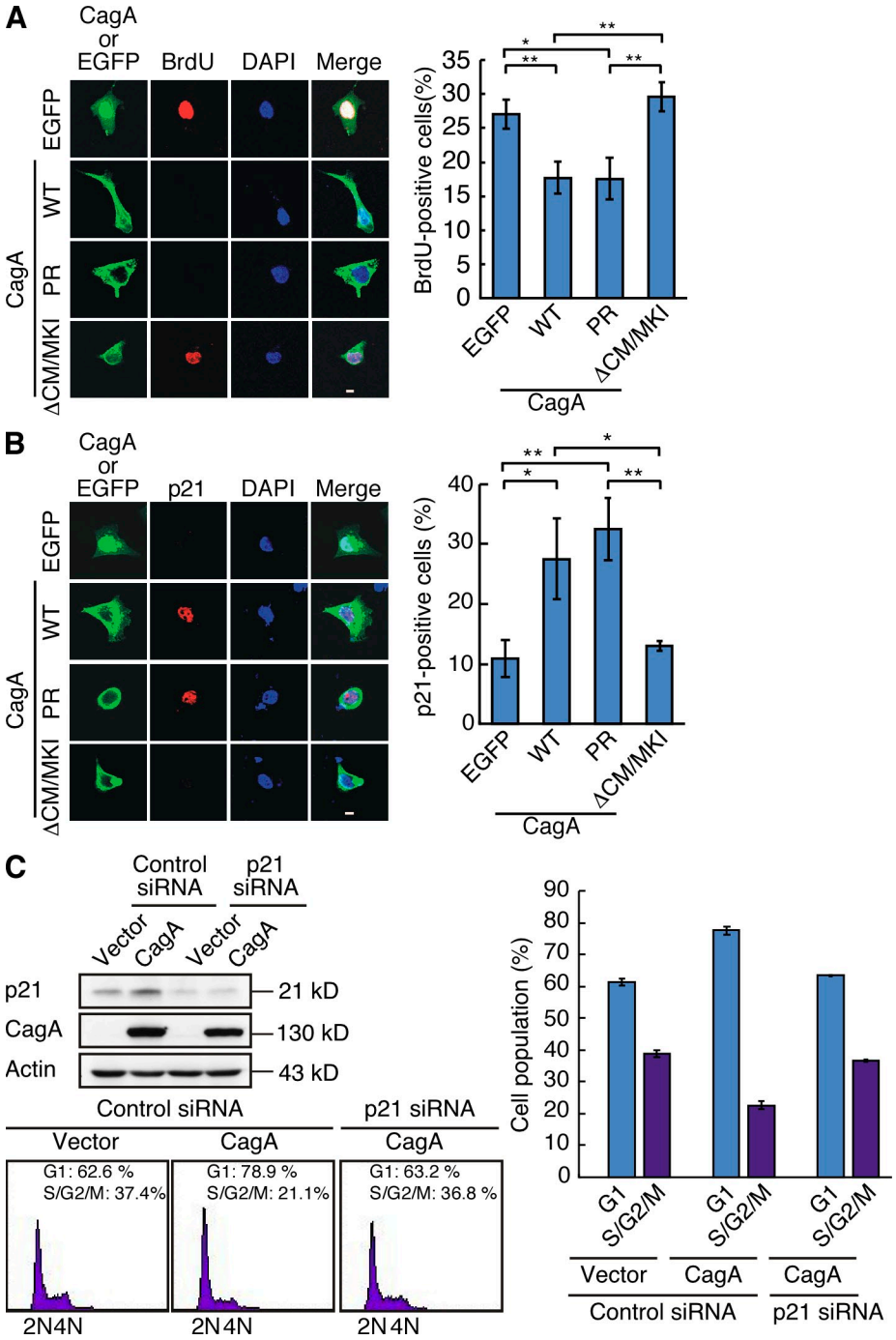

Figure S1. CagA inhibits cell proliferation by inducing p21 in nonpolarized AGS gastric epithelial cells. (A, left) AGS cells were transfected with an expression vector encoding HA-tagged WT CagA (WT), HA-tagged PR CagA (PR), HA-tagged CagA that lacks the CM/MKI (ΔCM/MKI), or EGFP as a control. At 27 h after transfection, cells were fixed and stained with anti-HA antibody (green) and anti-BrdU antibody (red). To visualize nuclei, cells were stained with DAPI (blue). Confocal x-y images are shown. Bar, 10 µm. (A, right) Percentage of BrdU-positive cells to AGS cells expressing CagA or EGFP (Student's *t* test). Error bars indicate mean ± SD. $n = 3$. **, $P < 0.01$; *, $P < 0.05$. (B, left) AGS cells were transfected with HA-tagged CagA (WT, PR, and ΔCM/MKI) or EGFP vector. At 27 h after transfection, cells were fixed and stained with anti-HA antibody (green), anti-p21 antibody (red), and DAPI (blue). Confocal x-y images are shown. Bar, 10 µm. (B, right) Percentage of p21-positive cells to AGS cells expressing CagA or EGFP (Student's *t* test). Error bars indicate mean ± SD. $n = 3$. **, $P < 0.01$; *, $P < 0.05$. (C, left) AGS cells were treated with a p21-specific siRNA and were then transiently transfected with an expression vector encoding EGFP or the GFP-CagA fusion protein (Yokoyama et al. 2005. *Proc. Natl. Acad. Sci. USA.* 101: 9661–9666). Cell lysates were subjected to immunoblotting with anti-HA, anti-p21, and anti-actin antibodies (top). Transfected cells were also stained with propidium iodide and EGFP- or GFP-CagA–positive cells were subjected to cell cycle analysis with flow cytometry (bottom). (C, right) Percentages of cells in G1 and S/G2/M cell cycle phases. Error bars indicate mean ± SD. $n = 3$. Representative staining and gel images from three independent experiments are shown in all panels.

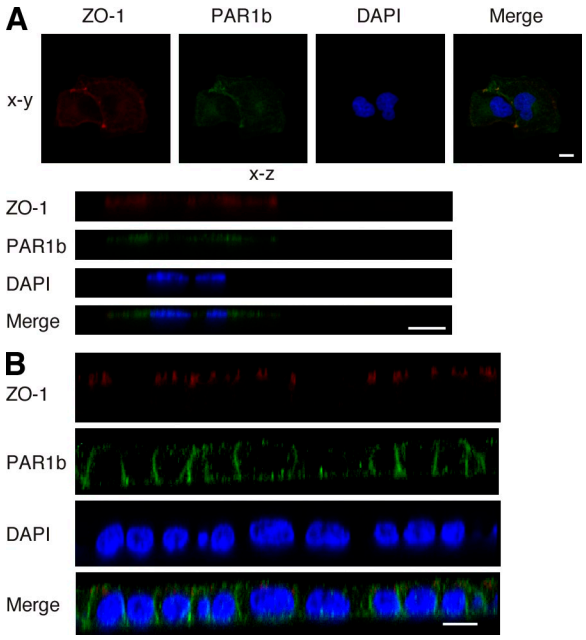

Figure S2. ZO-1 and PAR1b staining images of MDCK cells. (A) Nonpolarized MDCK cells were stained with anti–ZO-1 antibody (red), anti-PAR1b antibody (green), and DAPI (blue). Confocal x-y (top) and x-z (bottom) images are shown. Bars, 10 µm. (B) Polarized MDCK cells were stained with anti–ZO-1 antibody (red), anti-PAR1b antibody (green), and DAPI (blue). Confocal x-z images are shown. Bar, 10 µm. Representative staining images from three independent experiments are shown in all panels.

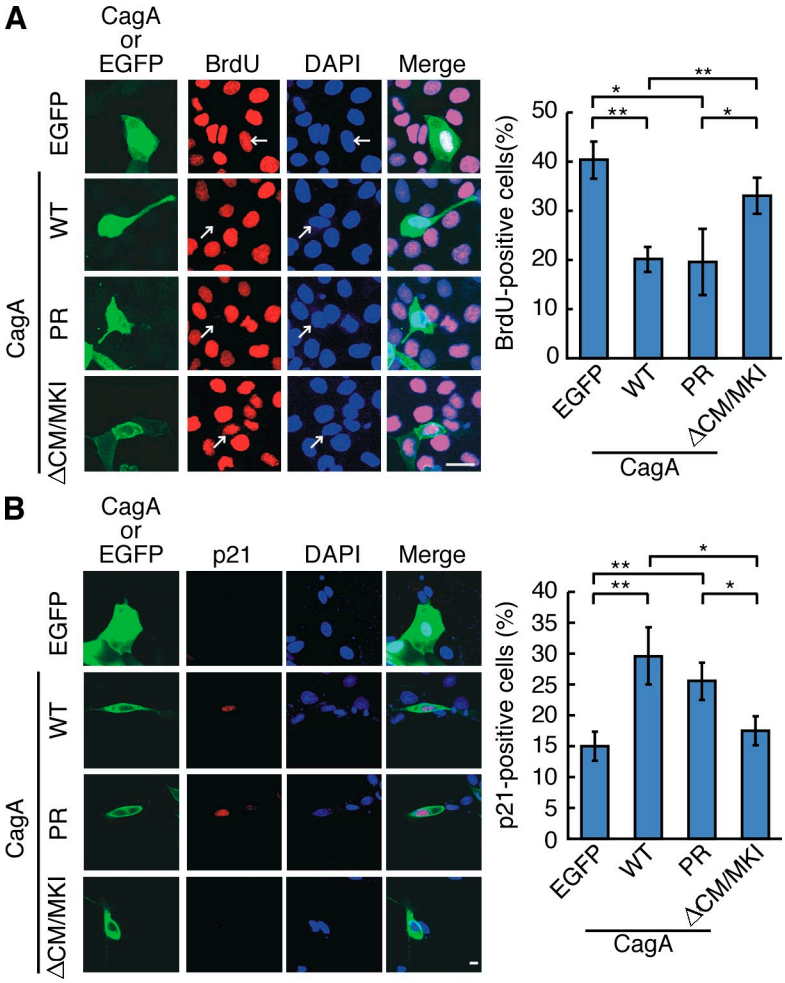

Figure S3. Inhibition of proliferation by CagA in nonpolarized MDCK cells. (A, left) Nonpolarized MDCK cells were transfected with HA-tagged CagA (WT, PR, and ΔCM/MKI) or EGFP vector. At 27 h after transfection, cells were fixed and stained with anti-HA antibody (green), anti-BrdU antibody (red), and DAPI (blue). White arrows in anti-BrdU or DAPI staining indicate positions of CagA- or EGFP-positive cells (nuclei). Confocal x-y images are shown. Bar, 10 µm. (A, right) Percentage of BrdU-positive cells to MDCK cells expressing CagA or EGFP (Student's *t* test). Error bars indicate mean ± SD. *n* = 3. **, P < 0.01; *, P < 0.05. (B, left) Nonpolarized MDCK cells were transfected with HA-tagged CagA (WT, PR, and ΔCM/MKI) or EGFP vector. At 27 h after transfection, cells were fixed and stained with anti-HA antibody (green), anti-p21 antibody (red), and DAPI (blue). Confocal x-y images are shown. Bar, 10 µm. (B, right) Percentage of p21-positive cells to MDCK cells expressing CagA or EGFP (Student's *t* test). Error bars indicate mean ± SD. *n* = 3. **, P < 0.01; *, P < 0.05. Representative staining images from three independent experiments are shown.

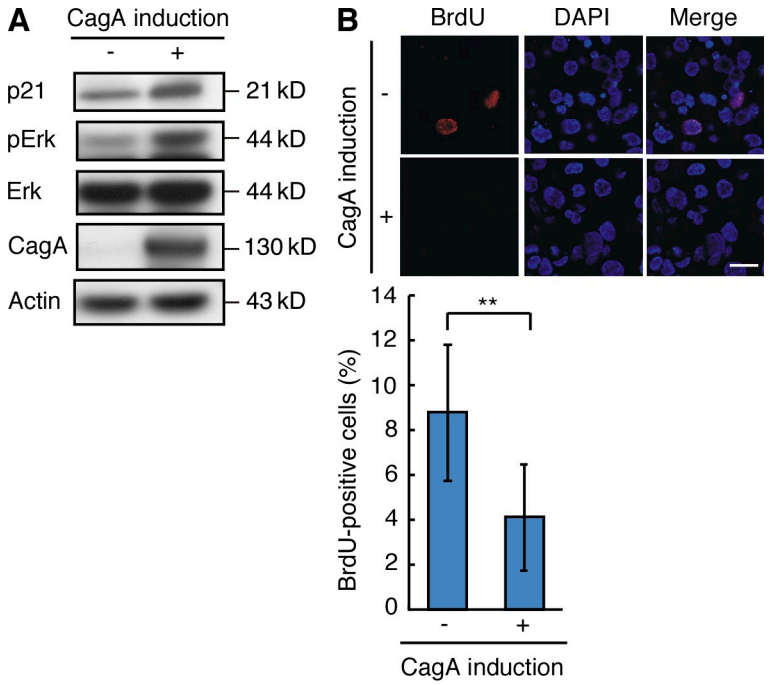

Figure S4. CagA induces p21 and inhibits cell proliferation in MKN28 cells cultured on Transwell filters. (A) MKN28-derived CagA-inducible WT-A10 cells were cultured on Transwell filters for 10 d in the presence of Dox (CagA induction −). Cells were then treated with (CagA induction −) or without (CagA induction +) Dox for 24 h. Cell lysates were immunoblotted with the indicated antibodies. (B, top) Nonpolarized WT-A10 cells were cultured on a Transwell filter for 10 d in the presence of Dox. CagA was then induced, as described in A, in the presence of 10 µM BrdU for 12 h. Cells were fixed and stained with anti-BrdU antibody (red) and DAPI (blue). Confocal x-y images are shown. Bar, 10 µm. (B, bottom) Percentage of BrdU-positive cells to total WT-A10 cells (Student's *t* test). Error bars indicate mean ± SD. $n = 3$. **, $P < 0.01$. Representative gel (A) and staining (B) images from three independent experiments are shown.

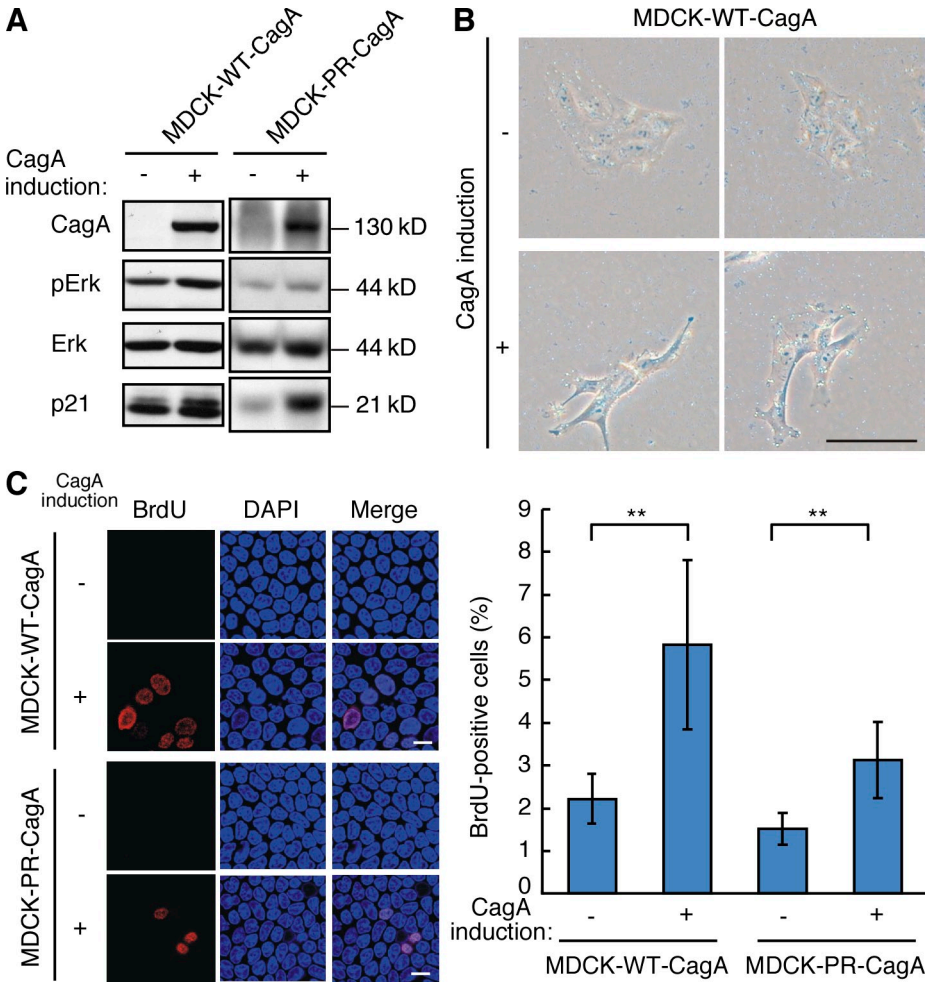

Figure S5. Establishment of MDCK-derived stable transfectants that inducibly express CagA by tet-on system. (A) A transfectant clone MDCK-WT-CagA inducibly expresses WT CagA, whereas another transfectant clone MDCK-PR-CagA inducibly expresses PR CagA in the presence of Dox. MDCK-WT-CagA and MDCK-PR-CagA cells were cultured in the absence or presence of Dox for 48 h and cell lysates prepared were immunoblotted with the indicated antibodies. (B) CagA-inducible MDCK-WT-CagA cells were cultured for 5 d in the presence or absence of Dox. Cells were washed, fixed with formaldehyde, and incubated overnight with the staining buffer to detect senescence-associated β-galactosidase activity. Light micrograph images are shown. Bar, 100 µm. (C, left) MDCK-WT-CagA and MDCK-PR-CagA cells were polarized by membrane filter culture. After induction of CagA with Dox, cells were labeled with BrdU for 15 h, fixed with paraformaldehyde, permeabilized with 0.5% Triton-X 100, and stained with anti-BrdU antibody (red) and DAPI (blue). Confocal x-y images are shown. Bars, 10 µm. (C, right) The percentage of BrdU-positive cells to total CagA-positive cells (Student's *t* test). Error bars indicate mean ± SD. $n = 3$. **, $P < 0.01$ Representative gel (A) and staining (B and C) images from three independent experiments are shown in all panels.

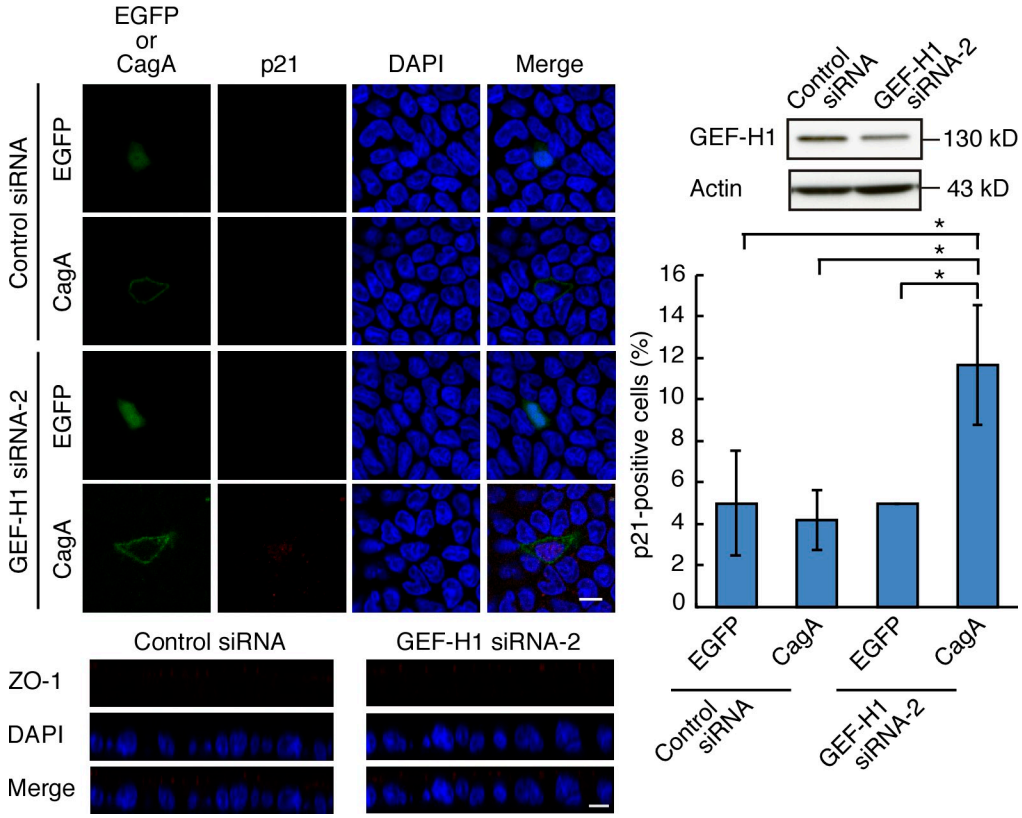

Figure S6. Requirement of GEF-H1 for the inhibition of CagA-mediated p21 accumulation in polarized epithelial cells. Polarized MDCK cells treated with GEF-H1 siRNA-2 or control siRNA (luciferase GL2) were transfected with CagA or EGFP expression vector. Cells were stained with anti-p21 antibody (red, top left, confocal x-y view) or anti–ZO-1 antibody (bottom left, confocal x-z view). Bars, 10 µm. Anti–GEF-H1 immunoblotting of polarized MDCK cells treated with GEF-H1 siRNA or control siRNA (top right). Percentage of p21-positive cells in GEF-H1-knockdown MDCK cells expressing CagA or EGFP. Error bars indicate mean ± SD. $n = 3$. *, $P < 0.05$ (bottom right). Representative staining and gel images from three independent experiments are shown.

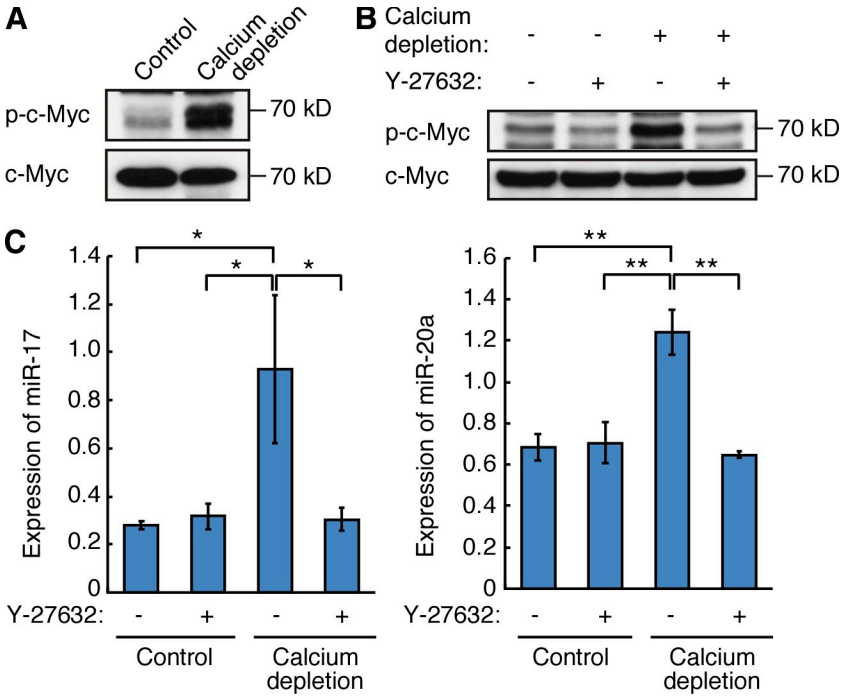

Figure S7. Induction of p21-targeting microRNAs upon calcium depletion by activating ROCK–c-Myc pathway in polarized epithelial cells. (A) Polarized MDCK cells were cultured in calcium-free medium for 24 h. Cell lysates were subjected to immunoblotting with indicated antibodies. Note that phospho-c-Myc (p-c-Myc) represents the active form of c-Myc. (B) Polarized MDCK cells were cultured in calcium-free medium for 24 h in the presence or absence of Y-27632. Cell lysates were immunoblotted with indicated antibodies. (C) Polarized MDCK cells were cultured in calcium-free medium (calcium depletion) or normal medium (control) for 24 h in the presence or absence of 50 µM Y-27632. Expression of miR-17 (left) or miR-20a (right) was measured by real-time PCR (Student's *t* test). Error bars indicate mean ± SD. $n = 3$. **, $P < 0.01$; *, $P < 0.05$. Representative gel images from three independent experiments are shown in A and B.

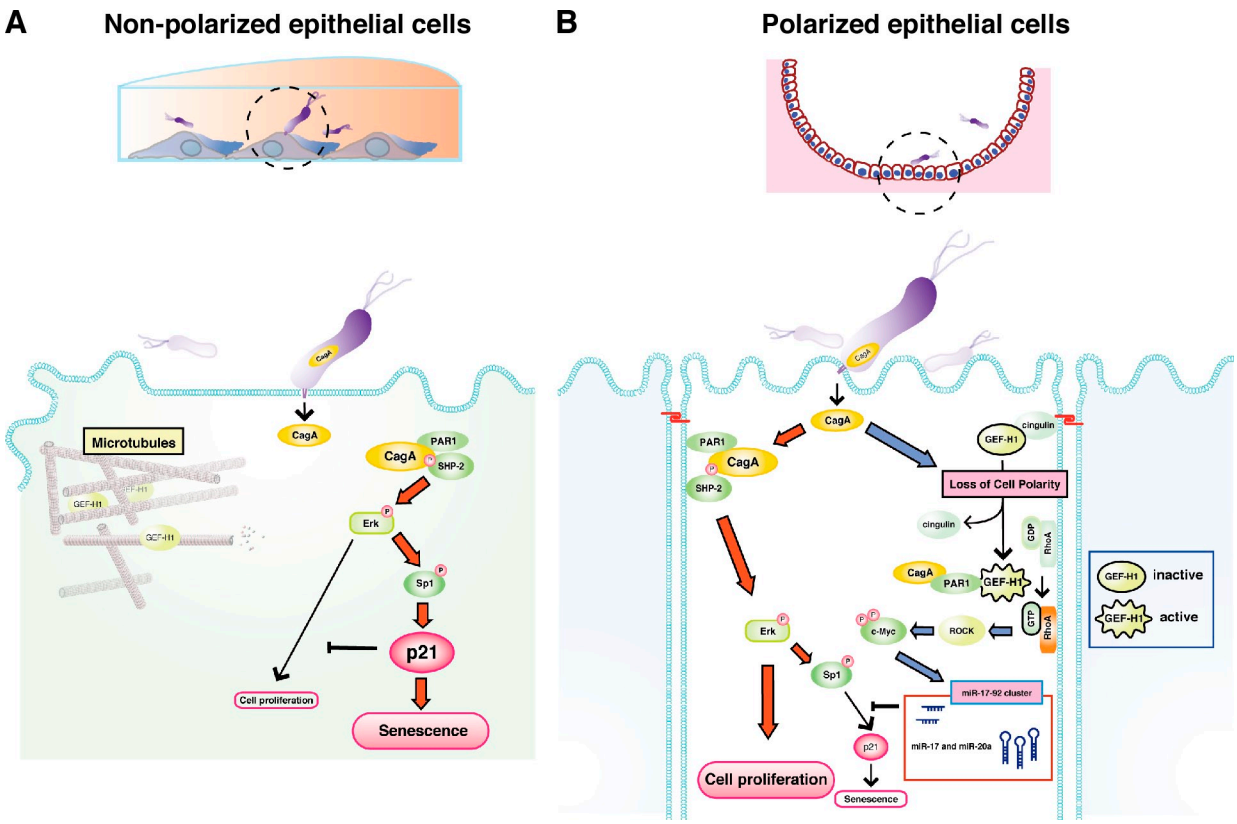

Figure S8. A model for epithelial polarity–dependent cellular response to CagA. *H. pylori* CagA is delivered into gastric epithelial cells via type IV secretion. Delivered CagA binds to and deregulates cellular proteins such as SHP-2 to elicit aberrant Erk activation. (A) In nonpolarized epithelial cells, CagA-activated Erk signaling induces p21 accumulation and subsequent cell senescence. In these cells, a RhoA-specific GDP/GTP exchange factor GEF-H1 is associated with microtubules and is thereby kept inactive in the cytoplasm. (B) In polarized epithelial cells, GEF-H1 is recruited to the tight junction, where it forms a complex with cingulin. Because cingulin is a GEF-H1 inhibitor, GEF-H1 is kept inactive in the complex. CagA delivered into polarized epithelial cells interacts with PAR1 and this CagA–PAR1 interaction induces junctional and polarity defects, which cause dissociation of GEF-H1 from cingulin. Once liberated from cingulin, GEF-H1 activates the RhoA–ROCK–c-Myc pathway to inhibit p21 accumulation by mechanisms that involve induction of Myc-regulated microRNAs that target *p21* mRNA. As a result, expression of CagA in polarized epithelial cells provokes Erk-dependent proliferation without causing p21 accumulation and subsequent cell senescence.